RIGA TECHNICAL UNIVERSITY

Ruslans Muhamadejevs

# PHYSICAL-CHEMICAL AND IN SILICO STUDIES OF 1,4-DIHYDROPYRIDINE DERIVATIVES

Summary of the Doctoral Thesis

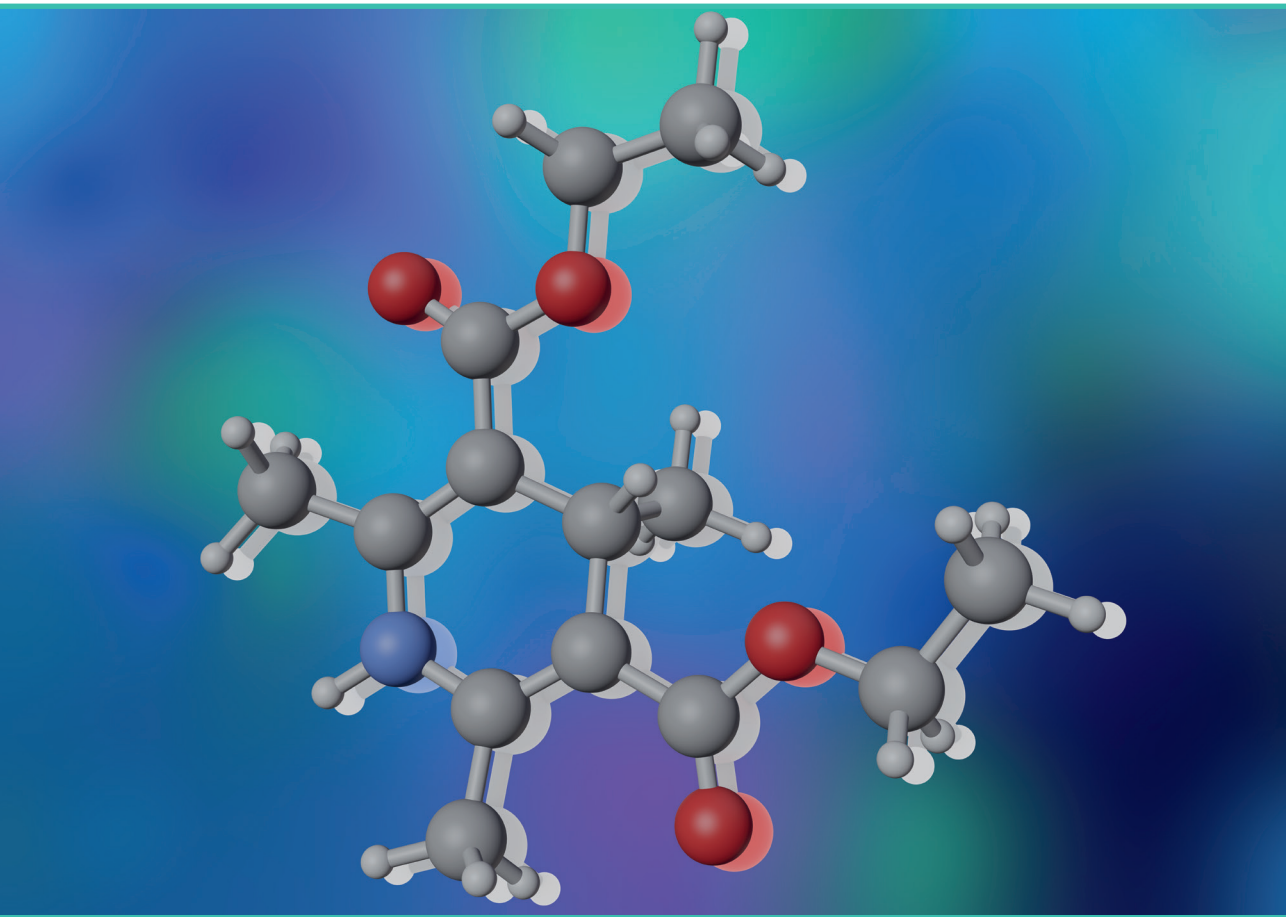

RTU Press
Riga 2023

**RIGA TECHNICAL UNIVERSITY**
Faculty of Materials Science and Applied Chemistry
Institute of Applied Chemistry

**Ruslans Muhamadejevs**
Doctoral Student of the Study Programme "Chemistry"

# PHYSICAL-CHEMICAL AND *IN SILICO* STUDIES OF 1,4-DIHYDROPYRIDINE DERIVATIVES

**Summary of the Doctoral Thesis**

Scientific supervisors

Dr. chem. Marina PETROVA

Associate Professor Dr. chem. Māra PLOTNIECE

Professor Dr. habil. chem. Edvards LIEPIŅŠ

Professor Dr. habil. chem. Valdis KAMPARS

RTU Press
Riga 2023

Muhamadejevs, R. Physical-chemical and *in silico* Studies of 1,4-dihydropyridine Derivatives. Summary of the Doctoral Thesis. Riga: RTU Press, 2023. 42 p.

Published in accordance with the decision of the Promotion Council "RTU P-01" of 23 March 2023, Minutes No. 04030-9.1/42.

Latvian Institute of Organic Synthesis


RTU
FACULTY OF MATERIALS SCIENCE AND APPLIED CHEMISTRY

Cover picture by Ruslans Muhamadejevs

https://doi.org/10.7250/9789934229138
ISBN 978-9934-22-913-8 (pdf)

# DOCTORAL THESIS PROPOSED TO RIGA TECHNICAL UNIVERSITY FOR THE PROMOTION TO THE SCIENTIFIC DEGREE OF DOCTOR OF SCIENCE

To be granted the scientific degree of Doctor of Science (Ph. D.), the present Doctoral Thesis has been submitted for the defence at the open meeting of RTU Promotion Council on June 19, 2023 at 14:00 at the Faculty of Materials Science and Applied Chemistry of Riga Technical University, 3 Paula Valdena Street, Room 272.

OFFICIAL REVIEWERS:

Senior Researcher Dr. chem. Artis Kinēns,
Latvian Institute of Organic Synthesis, Latvia

Assistant Professor Dr. chem. Agris Bērziņš,
University of Latvia, Latvia

Assistant professor Dr. chem. Raivis Žalubovskis,
Riga Technical University

## DECLARATION OF ACADEMIC INTEGRITY

I hereby declare that the Doctoral Thesis submitted for the review to Riga Technical University for the promotion to the scientific degree of Doctor of Science (Ph. D.) is my own. I confirm that this Doctoral Thesis had not been submitted to any other university for the promotion to a scientific degree.

Ruslans Muhamadejevs……. (signature)
Date: ……

The Doctoral Thesis has been written in Latvian. It consists of an Introduction, 3 chapters, Conclusions, 78 figures, 21 tables, 4 appendices; the total number of pages is 145. The Bibliography contains 328 titles.

# ANNOTATION

**Keywords:** 1,4-dihydropyridine derivatives, quantum chemical calculations, intramolecular hydrogen bonding, isothermal titration calorimetry, H/D isotope effects, nuclear magnetic resonance spectroscopy, bromination, *N*-bromosuccinimide.

The Doctoral Thesis is dedicated to the study of 1,4-dihydropyridine derivatives using nuclear magnetic resonance spectroscopy, Fourier transform infrared spectroscopy, isothermal titration calorimetry, and other physical-chemical methods as well as quantum chemical calculations. The Thesis consists of an introduction, a literature review, an evaluation of results, an experimental section, conclusions, a list of references and applications.

The bromination of the 2,6-dimethyl-1,4-dihydropyridine (1,4-DHP) derivatives with *N*-bromosuccinimide (NBS) leads to previously unknown intermediates that exist only in the reaction mixture. Their structures were identified by multinuclear ($^{1}$H, $^{13}$C and $^{15}$N) NMR spectral data.

An unusual temperature dependence of the diastereotopic protons of the AB system of the 2- and 6-methylene groups in the 1,4-DHP cycle was revealed by dynamic $^{1}$H NMR spectroscopy.

For the first time for some 1,4-DHP derivatives, an anomalous shortening of the |N-H| bond upon the intramolecular |N-H|···O hydrogen bond formation was registered by multinuclear NMR and IR spectroscopy.

By isothermal titration calorimetry and NMR technique, binding of 5'-mononucleotide monophosphates (as a prodrug model) to the lipid-like 1,4-dihydropyridine derivatives with long alkyl chains of the ester groups at positions 3 and 5 of the 1,4-DHP cycle (as potential candidate molecules for gene transfection systems) was characterized.

The Thesis is written in Latvian, its volume is 145 pages. It contains 78 figures, 21 tables, and 328 references.

# ACKNOWLEDGMENTS

I would like to express my deepest gratitude to my Thesis supervisors Dr. chem. Marina Petrova, Dr. hab. chem. Edvards Liepiņš, Dr. chem. Māra Plotniece, and Dr. hab. chem. Valdis Kampars for their scientific ideas, responsiveness, patience, support, and contribution during the development of the Doctoral Thesis.

Special thanks to Dr. chem. Laura Krasnova, Dr. chem. Brigita Vigante, Dr. chem. Aiva Plotniece, Dr. chem. Brigita Čekavičus, Dr. chem. Arkady Sobolev, Dr. chem. Kārlis Pajuste, Dr. chem. Gunārs Duburs, and other colleagues from the Laboratory of Membrane Active Compounds and β-diketones of the Latvian Institute of Organic Synthesis for synthesis compounds, scientific ideas and discussions.

My gratitude goes to Dr. chem. Juris Popelis for his significant help during the work and to the Head of the Laboratory of Physical Organic Chemistry of the Latvian Institute of Organic Synthesis, Dr. chem. Kristaps Jaudzems for his support.

I am very grateful to my family for patience and support during the development of the Doctoral Thesis.

# TABLE OF CONTENTS

ABBREVIATIONS ..... 7
GENERAL OVERVIEW OF THE THESIS ..... 8
Introduction ..... 8
Thesis objectives and tasks ..... 8
Scientific significance and novelty ..... 9
Practical significance ..... 9
Thesis statements to be defended ..... 9
Approbation of the research results ..... 10
MAIN RESULTS OF THE THESIS ..... 12
1. Bromination of methyl groups at positions 2 and 6 of 1,4-DHP cycle with NBS ..... 12
1.1. Bromination reaction of 1,4-DHP derivative 1a with one equivalent of NBS ... 13
1.2. Bromination reaction of 1,4-DHP derivative 1a with two equivalents of NBS . 14
1.3. Reaction kinetics of bromination of 1,4-DHP derivative 1a with NBS ..... 16
2. Structural properties of 1,4-DHP derivatives substituted at positions 2 and 6 ..... 18
2.1. 1,4-DHP derivatives with intramolecular hydrogen bonds of the type |H-C|···O=C ..... 19
2.2. 1,4-DHP derivatives with intramolecular hydrogen bonds of the type |N-H|···O=C ..... 23
3. Cationic lipids based on 1,4-DHP derivatives and their binding to mononucleotides ... 28
3.1. Studies of self-assembly of cationic amphiphilic lipid-like 1,4-DHP derivatives ..... 29
3.2. Binding of RNA 5'-mononucleotides to 1,4-DHP derivatives, $^{1}$H NMR titration ..... 30
3.3. Complexation of RNA 5'-mononucleotides with 1,4-DHP derivatives, comparison of the data obtained from $^{1}$H NMR and ITC studies ..... 31
3.4. Comparison of the formation of RNA 5'-mononucleotides complexes with the formation of complexes of some 1,4-DHP derivatives ..... 33
CONCLUSIONS ..... 36
REFERENCES ..... 38

# ABBREVIATIONS

| | |
|---|---|
| AMP | adenosine 5'-monophosphate |
| CMP | cytidine 5'-monophosphate |
| comp. | compound |
| CVC | critical vesicle concentration |
| DPPC | dipalmitoylphosphatidylcholine |
| FTIR | Fourier transform infrared |
| GMP | guanosine 5'-monophosphate |
| IE | isotope effect |
| IR | infrared |
| ITC | isothermal titration calorimetry |
| $K_D$ | dissociation constant |
| logP | octanol/water partition coefficient |
| NBS | *N*-bromosuccinimide |
| NHS | succinimide |
| NOE | nuclear Overhauser effect |
| PES | potential energy surface |
| ppb | parts per billion |
| ppm | parts per million |
| STDD | saturation transfer double difference |
| UMP | uridine 5'-monophosphate |

# GENERAL OVERVIEW OF THE THESIS

## Introduction

The 1,4-dihydropyridine (1,4-DHP) cycle is considered as one of the privileged structures in medicinal chemistry (1,4-DHP derivatives possess various pharmacological properties) [1,2] and 1,4-DHP derivatives are among the most important pharmaceutical products. For example, nifedipine and amlodipine are included in the World Health Organization (WHO) Model List of Essential Medicines [3]. Derivatives of 1,4-dihydropyridine not only possess properties of calcium channel antagonist and antihypertensive properties [4], but also antiarrhythmic [5], neurotransmitter [6], anticonvulsant [7], antioxidant [8], antiradical [9], anticancer [10], antidiabetic [11], antibacterial [12], cell growth modulator [13], anticoagulant [14], adenosine receptor antagonist [15], multidrug resistance modulator [16] and many other properties [1], [2].

1,4-DHP derivatives (cationic amphiphilic lipid-like compounds) with long alkyl chains have been synthesized at the Laboratory of Membrane Active Compounds and β-diketones of the Latvian Institute of Organic Synthesis. These derivatives exhibit self-assembly properties, form various types of vesicles in aqueous solutions, and can be used as non-viral gene transfection agents [17]. However, the mechanism of the complex formation of lipid-like cationic substituents containing 1,4-DHP derivatives with RNA/DNA is still unknown, and the self-assembling properties of these 1,4-DHP derivatives have not been well studied.

Similarly, 1,4-DHP derivatives containing cationic (pyridinium) substituents at positions 2 and 6 and carboxyl groups at positions 3 and 5 have not been fully characterized by physical chemistry and spectroscopic methods. As shown in the literature, some 1,4-DHP derivatives with the ketone groups at positions 3 and 5 have intramolecular hydrogen bonds, and the biological activity of 1,4-DHP derivatives is related to the type of conformers, the nature of the substituents and their mutual orientation [18].

## Thesis objectives and tasks

The aim of the Thesis is to characterize the geometrical properties of the structure of substituents at positions 2 and 6 of the 1,4-dihydropyridine cycle through experimental and theoretical studies using physico-chemical and *in silico* methods.

In order to achieve this goal, the following objectives were proposed:

1) to describe the reaction mechanism of the bromination of the methyl groups at positions 2 and 6 of 1,4-DHP derivatives by *N*-bromosuccinimide (NBS) in methanol;
2) to investigate the structural properties which cause the diastereotopy of the $CH_2$ group protons at the 2- and 6-positions of 2,6-bisbromomethyl-1,4-DHP derivatives;
3) to characterize the properties of intramolecular hydrogen bonds for various 1,4-DHP derivatives using NMR spectroscopy techniques and quantum chemical calculations;
4) to determine the thermodynamic parameters of the self-assembly of the vesicles obtained from lipid-like 1,4-DHP derivatives with long alkyl ester moieties and to characterize their interaction with mononucleotides as prodrug models.

## Scientific significance and novelty

Previously unknown intermediates in the bromination reaction of 2,6-dimethyl-1,4-dihydropyridine derivatives with *N*-bromosuccinimide have been identified and described. Insight into the mechanism of the bromination reaction was obtained.

Unusual temperature dependence of the diastereotopy of the protons of the AB system of the methylene groups at positions 2 and 6 of the 1,4-DHP cycle was observed and the existence of intramolecular hydrogen bonds in these molecules and the change of conformers depending on the temperature were demonstrated.

An anomalous shortening of the |N-H| bond when a hydrogen bond is formed was detected for some 1,4-DHP derivatives.

The interaction of the lipid-like 1,4-DHP derivatives with long alkyl ester groups with 5'-mononucleotide monophosphates was described by nuclear magnetic resonance spectroscopy and isothermal titration calorimetry.

## Practical significance

Studies of the bromination reaction of the methyl groups at positions 2 and 6 of the 1,4-dihydropyridine derivative in methanol with various amounts of *N*-bromosuccinimide provided an insight into the mechanism of the bromination reaction, so-far undescribed reaction intermediates were identified, the existence of which was confirmed by NMR spectroscopy. Quantum chemical calculations that describe the mechanism of this reaction were performed based on the obtained NMR spectroscopy results. The studies conducted allow the prediction of the reaction products and improve the synthesis yield.

For the lipid-like 1,4-DHP derivatives, binding to 5'-mononucleotide monophosphates, critical vesicle formation concentrations, and thermodynamic parameters were determined, which allow prediction of the binding capacity and the possibility of vesicle formation at low concentrations.

## Thesis statements to be defended

1. By brominating the methyl groups at positions 2 and 6 of 1,4-DHP with N-bromosuccinimide in methanol, previously undescribed products can be identified by NMR spectroscopy and confirmed using quantum chemical calculations.
2. In some 1,4-DHP derivatives the combined effect of magnetically anisotropic substituents and |C-H|···O type intramolecular hydrogen bonding in different conformers leads to significant difference in the shielding of the diastereotopic protons of the methylene group in positions 2 and 6, affecting their magnetic non-equivalence.
3. Characterization of intramolecular hydrogen bonds for various 2- or 2,6-substituted 1,4-DHP derivatives can be carried out by NMR and IR spectroscopy as well as by quantum chemical calculations.
4. NMR and isothermal titration calorimetry methods allow to study the ability of lipid-like 1,4-DHP derivatives to form complexes with 5'-mononucleotide monophosphates and to characterize the stability and binding interactions of the vesicle complexes formed.

## Approbation of the research results

The main results of the PhD Thesis have been published in four original scientific articles indexed in Scopus and Web of Science databases. In addition, the research results have been reported in 7 reports and presented at 6 conferences.

**Scientific publications**

1. **Muhamadejev, R.**; Petrova, M.; Smits, R.; Plotniece, A.; Pajuste, K.; Duburs, G.; Liepinsh, E. Study of interactions of mononucleotides with 1,4-dihydropyridine vesicles using NMR and ITC techniques. *New J. Chem*. **2018**, *42*, 6942–6948, doi:10.1039/C8NJ00160J.
2. Petrova, M.; **Muhamadejev, R.**; Vigante, B.; Duburs, G.; Liepinsh, E. Intramolecular hydrogen bonds in 1,4-dihydropyridine derivatives. *R. Soc. Open Sci.* **2018**, *5*, 180088, doi:10.1098/rsos.180088.
3. Petrova, M.; **Muhamadejev, R.**; Cekavicus, B.; Vigante, B.; Plotniece, A.; Sobolev, A.; Duburs, G.; Liepinsh, E. Experimental and Theoretical Studies of Bromination of Diethyl 2,4,6-Trimethyl-1,4-dihydropyridine-3,5-dicarboxylate. *Heteroat. Chem.* **2014**, *25*, 114–126, doi:10.1002/hc.21145.
4. Petrova, M.; **Muhamadejev, R.**; Chesnokov, A.; Vigante, B.; Cekavicus, B.; Plotniece, A.; Duburs, G.; Liepinsh, E. Spectral and Quantum-Chemical Study of Nonequivalence of Methylene Protons in 1,4-Dihydropyridine Derivatives*. *Chem. Heterocycl. Compd.* **2014**, *49*, 1631–1639, doi:10.1007/s10593-014-1414-6.

**Presentations at scientific conferences**

1. **Muhamadejev, R.**; Petrova, M.; Liepinsh, E. 11th Paul Walden Symposium, Diethyl 2,4,6-trimethyl-1,4-dihydropyridine-3,5-dicarboxylate bromination with N-bromosuccinimide. Theoretical and multinuclear NMR study of the reaction mechanism. D-10, Riga, Latvia, 19–20 September **2019**.
2. Petrova, M.; **Muhamadejev, R.**; Vigante, B.; Liepinsh, E. EUROISMAR2019 (EUROMAR 2019, ISMAR 2019), Intramolecular hydrogen bonds in 1,4-dihydropyridine derivatives. P366, Berlin, Germany, 25–30 August **2019**.
3. **Muhamadejev, R.**; Petrova, M.; Liepinsh, E. EUROISMAR2019 (EUROMAR 2019, ISMAR 2019), Theoretical and multinuclear NMR study of the reaction mechanism of diethy–l 2,4,6-trimethyl-1,4-dihydropyridine-3,5-dicarboxylate with N-bromosuccinimide. P313, Berlin, Germany, 25–30 August **2019**.
4. **Muhamadejev, R.**; Petrova, M.; Liepinsh, E. 10th Paul Walden Symposium, Intramolecular hydrogen bonds in 1,4-dihydropyridine derivatives. P-D6, Riga, Latvia, 15–16 June **2017**.
5. **Muhamadejev, R.**; Petrova, M.; Cekavicus, B.; Plotniece, A.; Duburs, G.; Liepinsh, E. Riga Technical University 57th International Scientific Conference “Materials Science and Applied Chemistry”, Binding of mononucleotides to 1,4-DHP vesicles, pp. 129–134, Riga, Latvia, 21–22 October **2016**.
6. **Muhamadejev, R.**; Vigante, B.; Petrova, M.; Duburs, G.; Liepinsh, E. Congress on the Heterocyclic Chemistry “KOST-2015”, Synthesis and structural characterization of 1,4-dihydropyridine derivatives with intramolecular hydrogen bond, P-060, Moscow, Russia, 18–23 October **2015**.

7. **Muhamadejev, R.**; Petrova, M.; Cekavicus, B.; Plotniece, A.; Duburs, G.; Liepinsh, E. Riga Technical University 55th International Scientific Conference, Section Material Science and Applied Chemistry, Experimental and in silico studies of self-assembling cationic and phospholipids. 30 p., Riga, Latvia 14–17 October **2014**.

# MAIN RESULTS OF THE THESIS

## 1. Bromination of methyl groups at positions 2 and 6 of 1,4-DHP cycle with NBS

Bromination of the methyl groups at positions 2 and 6 of the 1,4-DHP cycle is one of the most important steps in the development of cationic amphiphilic 1,4-DHP derivatives as potential candidates for gene transfection systems. Thus, the corresponding 2,6-bis(bromomethyl)-1,4-DHP derivatives further undergo nucleophilic substitution of the bromine atom with pyridine, its derivatives or other amines producing cationic amphiphiles. Very often, 2,6-bis(bromomethyl)-1,4-DHP is not even separated from the reaction medium, and used immediately *in situ* in a nucleophilic substitution reaction [19].

Bromination reactions of 1,4-DHP derivative **1a** with *N*-bromosuccinimide were carried out directly in NMR tubes (Ø 5 mm) in methanol solution and the NMR spectra were recorded during the reaction. It was found that the reactions proceeded in several steps (Figs. 1 and 2).

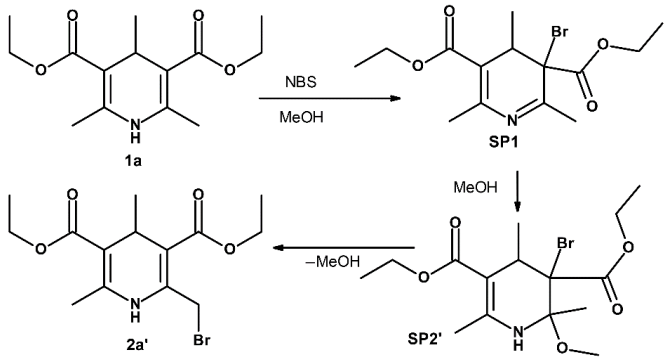


Fig. 1. Reaction scheme for the bromination of the methyl group of compound **1a** at position 2 of the 1,4-DHP cycle using one equivalent of NBS in methanol solution.

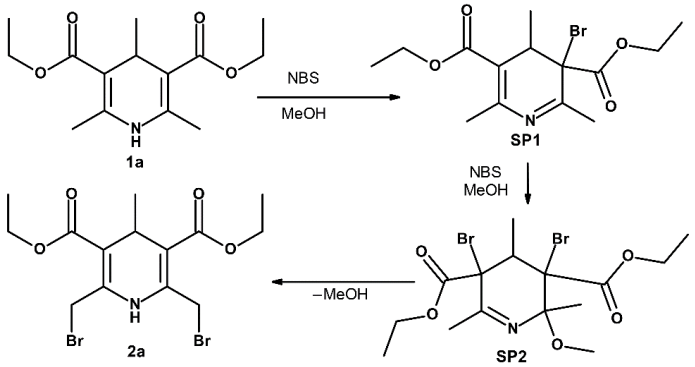


Fig. 2. Reaction scheme for the bromination of the methyl group of compound **1a** at position 2 of the 1,4-DHP cycle using two equivalents of NBS in methanol solution.

Intermediates **SP1**, **SP2** and **SP2'** were not isolated from the reaction mixture; however, they were stable enough to be identified by multinuclear ($^{1}$H, $^{13}$C and $^{15}$N) NMR spectroscopy, with assigning the proton, carbon, and nitrogen signals of intermediates **SP1**, **SP2**, **SP2'** and

the final products **2a'** and **2a**. The process of the formation of the intermediates and the products can be monitored by NMR spectroscopy. The $^{1}H$, $^{13}C$ and $^{15}N$ NMR chemical shifts for the intermediates are given in Table 1 (these data are partial, the full table is presented in Appendix 1 of the Thesis).

Table 1

$^{1}H$, $^{13}C$ and $^{15}N$ NMR data for the intermediates of the bromination reaction of 1,4-DHP derivative **1a** in methanol

| Comp. | $\delta^{1}H$, ppm | | | $\delta^{13}C$, ppm | | | | | $\delta^{15}N$, ppm |
|---|---|---|---|---|---|---|---|---|---|
| | $C_2$-R | $C_6$-R | $C_4H$ | $C_2$ | $C_3$ | $C_4$ | $C_5$ | $C_6$ | $N_1$ |
| **1a** | 2.23 | 2.23 | 3.77 | 146.18 | 102.96 | 28.09 | 102.96 | 146.18 | 135.21 |
| **SP1** | 2.38 | 2.48 | 3.35 | 165.29 | 59.44 | 38.44 | 116.75 | 150.56 | 311.35 |
| **SP2'** | 1.84 | 2.26 | 3.54 | 86.63 | 65.22 | 39.66 | 97.78 | 149.21 | 112.82 |
| **SP2** | 2.17 | 1.63 | 3.03 | 157.01 | 66.85 | 43.69 | 73.38 | 91.38 | 325.15 |
| **2a'*** | 4.44, 4.71 | 2.26 | 3.81 | 144.71 | 105.10 | 28.34 | 102.40 | 146.49 | 130.12 |
| **2a*** | 4.88, 4.51 | 4.88, 4.51 | 3.89 | 142.12 | 106.77 | 29.37 | 106.77 | 142.12 | 126.20 |

* Spectra were recorded in deuterated chloroform.

### 1.1. Bromination reaction of 1,4-DHP derivative 1a with one equivalent of NBS

Immediately after mixing of an equimolar amount of 1,4-DHP derivative **1a** with NBS, the only compound observed by NMR spectroscopy in the solution was intermediate **SP1**. The proposed mechanism for the bromination reaction of 1,4-DHP derivative **1a** with one equivalent of NBS in methanol is shown in Fig. 3.

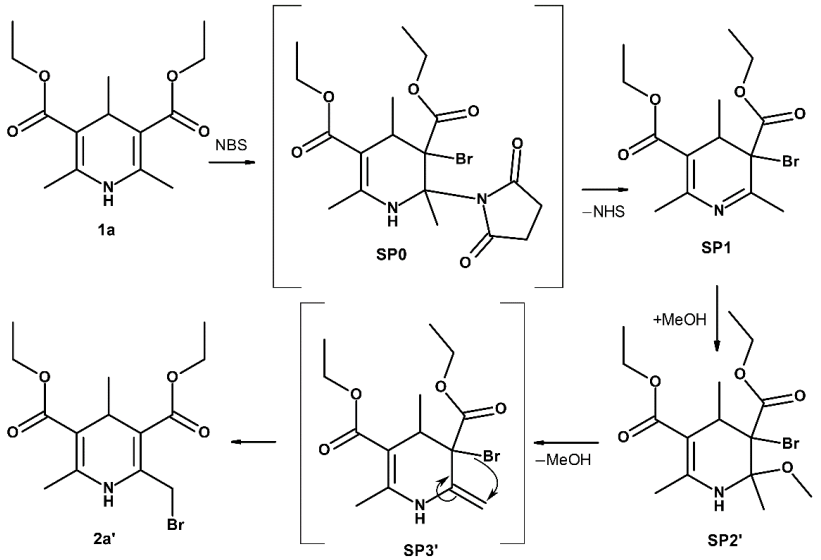


Fig. 3. Proposed reaction mechanism for the bromination of 2,4,6-trimethyl-1,4-dihydropyridine (**1a**) with one equivalent of NBS.

The first step is the reaction of 1,4-DHP derivative **1a** with NBS, where the possible intermediate **SP0** is formed, which is similar to the bromine and succinimide (NHS) adduct, described by Masson and co-workers [20]. Then rapid elimination of NHS leads to the formation of intermediate **SP1**. Next, methanol is attached to the $N_1$=$C_2$ bond of the **SP1** molecule, forming intermediate **SP2'**. Similar observations have been described for

chlorination reactions [21]. It can be assumed that the transformation of intermediate product **SP2'** to **2a'** occurs with the separation of a methanol molecule from compound **SP2'**, forming the possible corresponding intermediate **SP3'**, followed by [1,3]-sigmatropic rearrangement to monobromated product **2a'**.

To confirm this reaction mechanism, quantum chemical calculations were performed (Jaguar 8.0 software package [22]. Calculations were performed at the HF/LACV3P**++ level of theory) to determine the optimal structure of the intermediates and to estimate the internal energies of all intermediates involved in the reaction as well as their relative energy changes during a reaction. A schematic representation of the possible reaction using the relative energies of the reactants is shown in Fig. 4. The plot is scaled based on the relative energies as shown on the Y-axis.

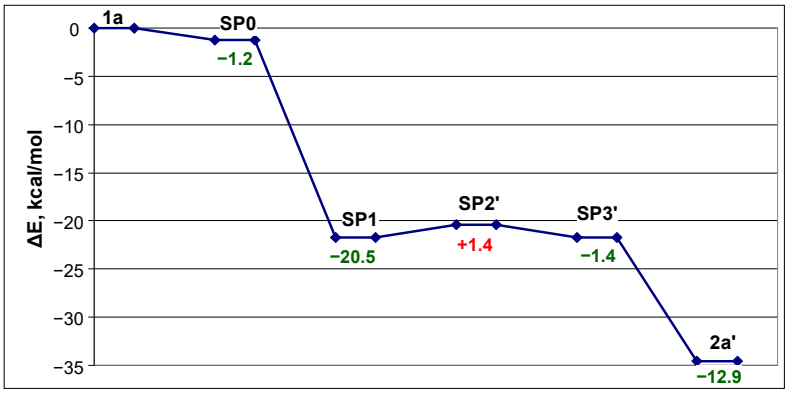


1) **1a**+ **NBS**→**SP0** $\Delta E$ = **−1.2** kcal/mol
2) **SP0** → **SP1** + **NHS** $\Delta E$ = **−20.5** kcal/mol
3) **SP1** + **MeOH** → **SP2'** $\Delta E$ = **+1.4** kcal/mol
4) **SP2'** → **SP3'** + **MeOH** $\Delta E$ = **−1.4** kcal/mol
5) **SP3'** → **2a'** $\Delta E$ = **−12.9** kcal/mol

Fig. 4. Energy diagram for the bromination reaction of compound **1a** with one equivalent of NBS, which is based on quantum chemical calculations.

The calculated internal energy differences of the bromination reaction steps show that addition of NBS to **1a** favours the formation of intermediate **SP0**. This process is favourable ($\Delta E$ = −1.2 kcal/mol). The elimination of NHS fragment from intermediate **SP0** and the formation of intermediate **SP1** thermodynamically are very favourable according to the quantum chemical calculations with an energy difference of −20.5 kcal/mol. The subsequent addition of methanol to form intermediate **SP1** and intermediate **SP2'** is slightly thermodynamically unfavourable and requires energy of 1.4 kcal/mol. This results in a relatively long stability of intermediates **SP1** and **SP2'**. According to the proposed bromination mechanism, the conversion of intermediate **SP2'** to product **2a'** occurs with the formation of intermediate **SP3'** ($\Delta E$ = −1.4 kcal/mol), followed by [1,3]-sigmatropic rearrangement. The final step **SP3'** → **2a'** was found to be energetically very favourable ($\Delta E$ = −12.9 kcal/mol).

### 1.2. Bromination reaction of 1,4-DHP derivative 1a with two equivalents of NBS

The proposed reaction mechanism for the bromination of compound **1a** with two equivalents of NBS in methanol is shown in Fig. 5. In the reaction of compound **1a** with two equivalents of NBS, the first and the second steps are the same as in the case of monobromination – the formation of intermediate **SP1**. The next step involves the addition of

a molecule of NBS to intermediate **SP1** to form the putative intermediate **SP1'**. Next, the addition of a methanol molecule to **SP1'** takes place with the subsequent release of NHS – the formation of **SP2**. Further removal of a methanol molecule from intermediate **SP2** results in the formation of intermediate **SP3**. This is followed by a [1,3]-sigmatropic rearrangement of intermediate **SP3** → **SP4**. The next step is the formation of the exocyclic double bond and then the rearrangement of **SP4** → **SP5** and **SP5** → **2a**.

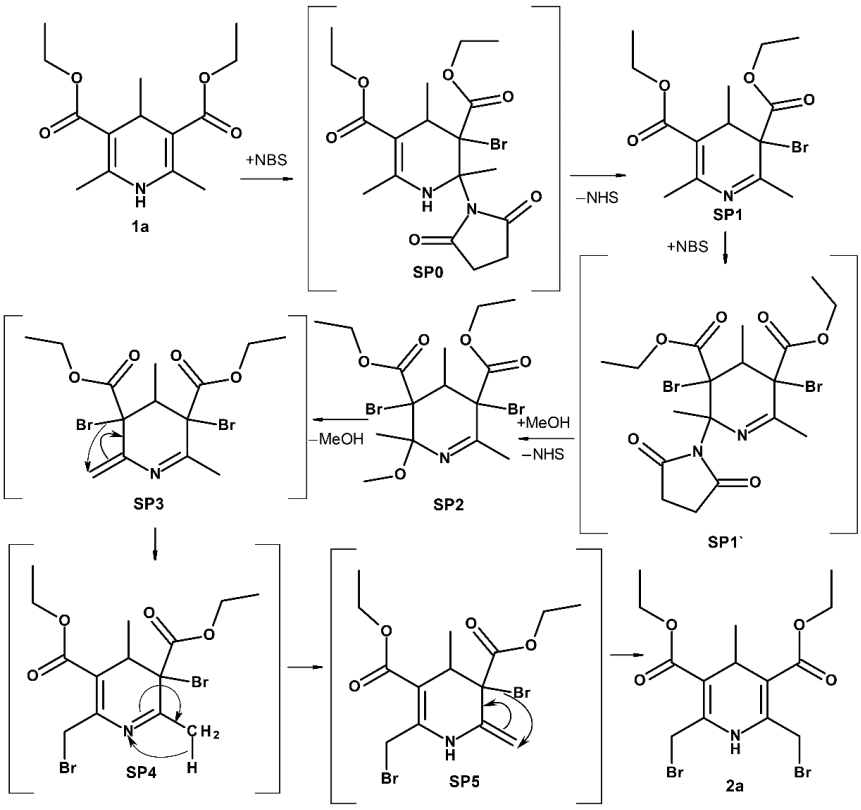


Fig. 5. Proposed reaction mechanism for the bromination of 2,4,6-trimethyl-1,4-dihydropyridine (**1a**) with two equivalents of NBS.

As in the case of the previous bromination with one equivalent of NBS, the steps of the transformations were determined by NMR and compared with the results of the quantum chemical calculations. In Fig. 6, the data show the relative energies of the intermediates involved in the different steps of the bromination process. The first two steps (formation of intermediate **SP1** *via* intermediate **SP0**) occur in the same way as in the case of monobromination reaction (Figs. 3 and 4). The next step is the addition of NBS molecule to intermediate **SP1**, where intermediate **SP1'** is formed. This process is energetically less favourable ($\Delta E$ = –2.2 kcal/mol). The next step is thermodynamically favourable ($\Delta E$ = −16.9 kcal/mol) and involves the addition of a methanol molecule to intermediate **SP1'** with the subsequent release of NHS, leading to intermediate **SP2**. Further removal of the methanol molecule from intermediate **SP2** is slightly energetically unfavourable ($\Delta E$ = +0.1 kcal/mol), resulting in the formation of intermediate **SP3**. The next steps are

[1,3]-sigmatropic rearrangements, where the bromine atom migrates to the exocyclic double bond, leading to the formation of the corresponding intermediate **SP4**. The calculation shows that the conversion **SP3** → **SP4** is energetically favourable ($\Delta E$ = −16.1 kcal/mol). The transition from intermediate **SP4** to product **2a** occurs to form the corresponding intermediate **SP5** ($\Delta E$ = +1.3 kcal/mol), followed by a second [1,3]-sigmatropic rearrangement. The final step, the formation of dibromo product **2a**, is energetically favourable ($\Delta E$ = −12.9 kcal/mol).

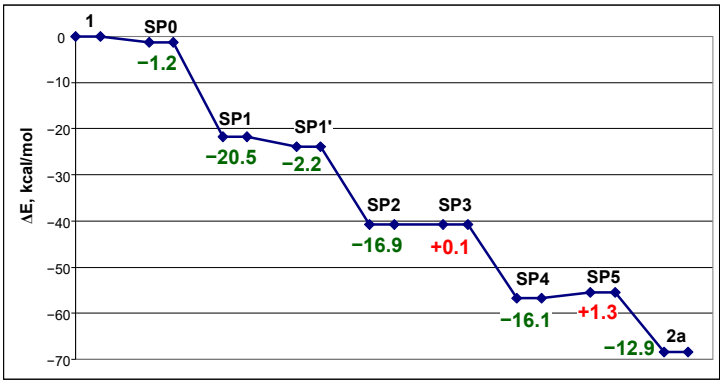


Fig. 6. Energy diagram for the bromination reaction of 2,4,6-trimethyl-1,4-dihydropyridine **1a** with two equivalents of NBS, which is obtained based on quantum chemical calculations.

### 1.3. Reaction kinetics of bromination of 1,4-DHP derivative 1a with NBS

The changes in the concentrations of the intermediates during the bromination reaction of 1,4-dihydropyridine derivative **1a** with one or two equivalents of NBS are presented in Fig. 7. It is important to note that the rate of formation of intermediate **SP2** (or **SP2'** in the case of one equivalent of NBS) matches the rate of decrease in the concentration of intermediate **SP1** (the changes in concentration are completely symmetrical). This observation indicates that the reaction is very fast and that most likely NBS is directly involved in this reaction as a promoter and not only as a source of bromine.

The bromination of 1,4-dihydropyridine derivative **1a** with two equivalents of NBS shows an asymmetric decrease in the concentration of intermediate **SP2** relative to the formation of the final product **2a** (increase in concentration). It is important to note that the decrease in the concentration of intermediate **SP2** is much faster than the formation of the final product **2a**. The transition of **SP2** starts only after **SP1** has completely reacted with NBS. There is also a period during the reaction when intermediate **SP2** is no longer detected in the solution but the final product **2a** is not yet fully formed. According to the calculation results, this slow formation of the final product is due to the existence of the energetically unfavourable transitions between intermediates (**SP2** → **SP3** and **SP4** → **SP5**), which causes a delay in the formation of the final brominated product **2a** (Fig. 7).

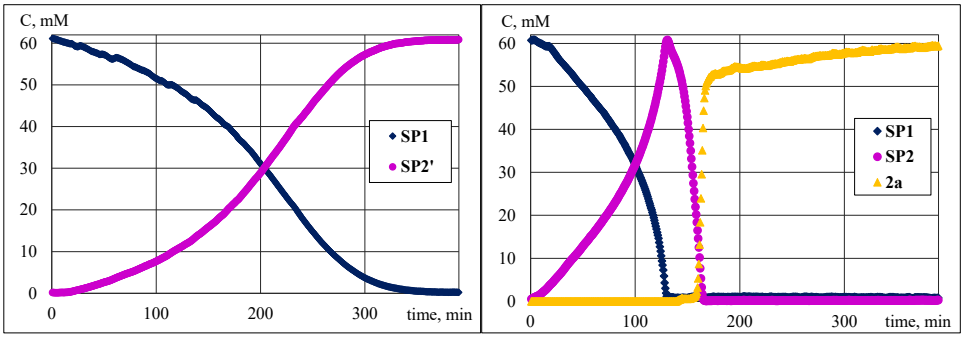


Fig. 7. Changes in compound concentration during the bromination reaction of 1,4-DHP derivative **1a** with one (on the left) and two (on the right) equivalents of NBS in methanol at 25 °C, observed by $^1$H NMR spectroscopy.

Looking at the energetic possibility of the formation of intermediate **SP1**, the question arises why the corresponding intermediate **SP2'** is not observed in the case of dibromination, as it was found in the case of monobromination. The reason could be that the addition of a methanol molecule to the $N_1$=$C_2$ double bond in intermediate **SP1** to form intermediate **SP2'** ($\Delta E$ = +1.4 kcal/mol) was shown to be thermodynamically slightly unfavourable (Fig. 4). In the presence of an excess of NBS, it is more likely that intermediate **SP1** would attach NBS molecule to the $C_5$=$C_6$ double bond of the 1,4-DHP cycle and then replace it with methanol. According to the calculations, these two steps **SP1** → **SP1'** → **SP2** ($\Delta E$ = –19.1 kcal/mol) (Fig. 6) are energetically more favourable than **SP1** → **SP2'** ($\Delta E$ = +1.4 kcal/mol) (Fig. 4). That ensures the formation of intermediate **SP2** and also accelerates the reaction when two or more equivalents of NBS are used (Fig. 8).

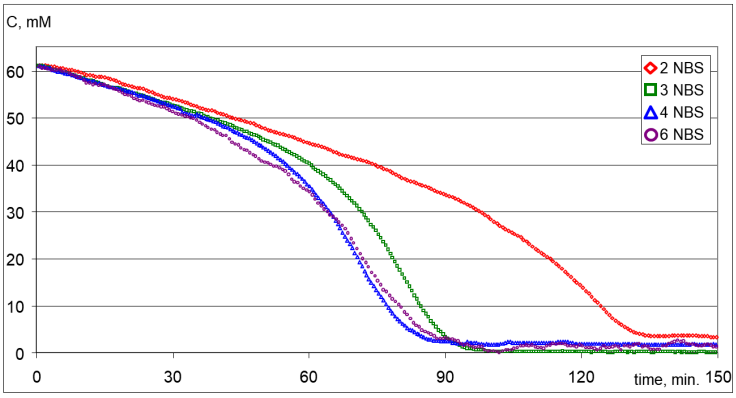


Fig. 8. The changes in the concentration of intermediate **SP1** observed by $^1$H NMR spectroscopy during the bromination reaction of compound **1a** with different equivalent ratios of NBS in methanol at 25 °C.

The experimental results show that with an increase in the concentration of NBS, starting from two equivalents, the initial intermediates in the bromination reaction are the same as in reaction with two NBS equivalents and increases the rate of transformation of intermediates **SP1** to **SP2**. In the bromination reaction mixtures of 1,4-DHP derivative **1a** with two and more

equivalents of NBS, no presence of intermediate **SP2'** was observed, and only in the case of the reaction with one equivalent of NBS some traces of intermediate **SP2** were observed.

## 2. Structural properties of 1,4-DHP derivatives substituted at positions 2 and 6

Over the last 30 years, a large number of studies have been reported attempting to modify the methyl groups at positions 2 and 6 of 1,4-DHP cycle with various substituents [12], [17], [23]–[27]. Also, the cationic amphiphilic 1,4-DHP derivatives have gained an increased attention as promising transport molecules for the delivery of nucleotides into target cells [19].

The research carried out during the MSc studies [28] was continued during the development of the Doctoral Thesis. All investigated compounds were synthesized in the Laboratory of Membrane Active Compounds and β-diketones at the Latvian Institute of Organic Synthesis (Table 2).

Table 2

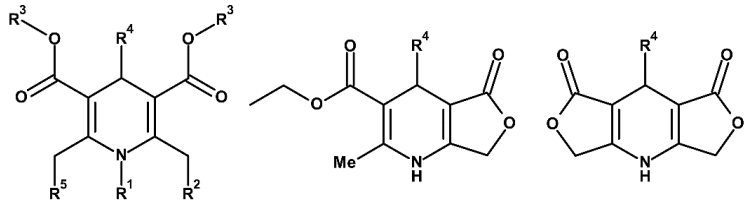


Chemical structures of the 1,4-DHP derivatives **1–8**

| No. | Comp. | $R^1$ | $R^2$ | $R^3$ | $R^4$ | $R^5$ |
|---|---|---|---|---|---|---|
| 1. | **1a** | H | H | $CH_2CH_3$ | $CH_3$ | H |
| 2. | **1b** | H | H | $CH_2CH_3$ | Ph | H |
| 3. | **1c** | H | H | $(CH_2)_2OC_3H_7$-*n* | $PhOCHF_2$-*o* | H |
| 4. | **2a**** | H | Br | $CH_2CH_3$ | $CH_3$ | Br |
| 5. | **2b*** | $CH_3$ | Br | $CH_2CH_3$ | Ph | Br |
| 6. | **2c**** | H | Br | $CH_2CH_3$ | $PhCF_3$-*o* | Br |
| 7. | **2d**** | H | Br | $(CH_2)_2OC_3H_7$-*n* | $PhOCHF_2$-*o* | Br |
| 8. | **2e**** | H | Cl | $CH_2CH_3$ | $COOCH_3$ | Cl |
| 9. | **2f*** | H | Br | $CH_2CH_3$ | Ph | Br |
| 10. | **2g**** | H | Br | $CH_3$ | $PhOCHF_2$-*o* | Br |
| 11. | **2h**** | H | Br | $C_{12}H_{25}$ | Ph | Br |
| 12. | **2i**** | $CH_3$ | Br | $CH_3$ | $PhOCHF_2$-*o* | Br |
| 13. | **3a*** | H | $Py^+ Br^-$ | $CH_2CH_3$ | $CH_3$ | $Py^+ Br^-$ |
| 14. | **3b*** | $CH_3$ | $Py^+ Br^-$ | $CH_2CH_3$ | Ph | $Py^+ Br^-$ |
| 15. | **3c**** | H | $Py^+ Br^-$ | $CH_2CH_3$ | $PhCF_3$-*o* | $Py^+ Br^-$ |
| 16. | **3d**** | H | $Py^+ Br^-$ | $(CH_2)_2OC_3H_7$-*n* | $PhOCHF_2$-*o* | $Py^+ Br^-$ |
| 17. | **3e**** | H | $Py^+ Cl^-$ | $CH_2CH_3$ | $COOCH_3$ | $Py^+ Cl^-$ |
| 18. | **3f**** | H | $Py^+ Br^-$ | $CH_2CH_3$ | Ph | $Py^+ Br^-$ |
| 19. | **3g*** | H | $Py^+ Br^-$ | $CH_3$ | $PhOCHF_2$-*o* | $Py^+ Br^-$ |
| 20. | **3h**** | $CH_3$ | $Py^+ Br^-$ | $CH_3$ | $PhOCHF_2$-o | $Py^+ Br^-$ |
| 21. | **4a**** | H | $Py^+ Br^-$ | $C_{10}H_{21}$ | Ph | $Py^+ Br^-$ |
| 22. | **4b*** | H | $Py^+ Br^-$ | $C_{12}H_{25}$ | Ph | $Py^+ Br^-$ |
| 23. | **4c**** | H | $Py^+ Br^-$ | $C_{14}H_{29}$ | Ph | $Py^+ Br^-$ |
| 24. | **4d*** | H | $Py^+ Br^-$ | $C_{16}H_{33}$ | Ph | $Py^+ Br^-$ |
| 25. | **4e*** | $CH_3$ | $Py^+ Br^-$ | $C_{12}H_{25}$ | Ph | $Py^+ Br^-$ |
| 26. | **4f*** | H | $Py^+CH_3$-*4* $Br^-$ | $C_{12}H_{25}$ | Ph | $Py^+CH_3$-*4* $Br^-$ |
| 27. | **4g*** | H | $Py^+(CH_3)_2$-*3,5* $Br^-$ | $C_{12}H_{25}$ | Ph | $Py^+(CH_3)_2$-*3,5* $Br^-$ |
| 28. | **4h*** | H | $Py^+(N\text{-}(CH_3)_2)$-*4* $Br^-$ | $C_{12}H_{25}$ | Ph | $Py^+(N\text{-}(CH_3)_2)$-*4* $Br^-$ |
| 29. | **4i*** | H | $Py^+ Br^-$ | $C_{12}H_{24}$-$CF_3$ | Ph | $Py^+ Br^-$ |

Table 2 (continued)

| No. | Comp. | $R^1$ | $R^2$ | $R^3$ | $R^4$ | $R^5$ |
|---|---|---|---|---|---|---|
| 30. | **4j*** | H | $Py^+ Br^-$ | $C_{12}H_{25}$ | Ph-$CF_3$-*p* | $Py^+ Br^-$ |
| 31. | **5a** | H | $OOCCH_3$ | $CH_2CH_3$ | $CH_3$ | H |
| 32. | **5b** | H | $OOCCH_3$ | $CH_3$ | $CH_3$ | H |
| 33. | **5c** | H | $OOCCH_3$ | $CH_2CH_3$ | Ph | H |
| 34. | **5d** | H | $OOCCH_3$ | $(CH_2)_2OC_3H_7$-*n* | PhO$CHF_2$-*o* | H |
| 35. | **5e** | H | $OOCCH_3$ | $CH_2CH_3$ | Ph-F-*o* | H |
| 36. | **5f** | H | $OOCCH_3$ | $CH_2CH_3$ | Ph-$NO_2$-*m* | H |
| 37. | **6a** | H | $OOCCH_3$ | $CH_2CH_3$ | $CH_3$ | $OOCCH_3$ |
| 38. | **6b** | H | $OOCCH_3$ | $CH_2CH_3$ | Ph | $OOCCH_3$ |
| 39. | **6c** | H | $OOCCH_3$ | $(CH_2)_2OC_3H_7$-*n* | PhO$CHF_2$-*o* | $OOCCH_3$ |
| 40. | **7a**** | | | | Ph | |
| 41. | **7b**** | | | | PhO$CHF_2$-*o* | |
| 42. | **8a*** | | | | Ph | |
| 43. | **8b*** | | | | PhO$CHF_2$-*o* | |

* – the compound was previously described in the MSc Thesis [28].

** – the compound was previously described in the publication [29], written on the basis of the data obtained during the MSc studies, but it was not described in the MSc thesis.

The table uses a special numbering for the compounds because they are divided into different groups.

The $CH_2X$ protons of the methylene groups substituted at positions 2 and 6 of the 1,4-dihydropyridine cycle have an interesting property (compounds **2–6** (Table 2) – they are diastereotopic. In the corresponding $^1$H NMR spectra these protons are observed as AB spin systems. This nonequivalence may be affected by both the conformation and the anisotropy of the substituents of the molecule.

The substituent at position 4 of the 1,4-DHP cycle is located at a considerable distance from the methylene groups at positions 2 and 6 of the molecule. Therefore, the experimentally observed difference in the $^1$H NMR chemical shifts of the protons in the $CH_2$ group of the cyclic lactones **7** and **8** does not exceed 0.08 ppm. A similar difference has been reported in the literature for 1,4-DHP derivatives, and it is clear that the $CH_2$ group has diastereotopic properties only when the 1,4-DHP cycle is not oxidized because in the $^1$H NMR spectra of pyridine derivatives, the proton signals of the $CH_2$ group are observed as singlets [30].

Another important factor of the anisotropy in the monocyclic derivatives **2**–**6** could be the conformation of the 3,5-alkoxycarbonyl groups. In these compounds, the difference in chemical shifts for $CH_2X$ protons becomes significant. It can be assumed that the chemical shift difference in compounds **2**–**6**, caused by the anisotropy of the substituents at position 4 of the 1,4-DHP cycle, is additionally influenced by the difference in the position of the protons relative to the 3,5-alkoxycarbonyl substituent.

### 2.1. 1,4-DHP derivatives with intramolecular hydrogen bonds of the type |H-C|···O=C

The AB proton signals of the methylene groups at positions 2 and 6 of the 1,4-DHP cycle of compounds **2**–**6** in the $^1$H NMR spectra can be easily identified by the characteristic 11–15 Hz high geminal ($^2J$) spin-spin coupling constants. For compound **2** the constant is smaller than for compounds **3–8**. The adjacent pyridine π bonds in derivatives **3** and **4** generally cause an increase in the absolute value of the $^2J$ constant.

Analysis of the nuclear Overhauser effect (NOE) in the $^1$H-$^1$H NOESY spectra of compounds **2**–**4** allows the relative position of the AB protons of the methylene group to be determined – the correlation signal of the NOE for the transfer from the $N_1$ proton to the more

strongly shielded proton $H_A$ is twice as intense as for the transfer to $H_B$ [29]. This means that the $H_A$ proton, which resonates in the lower frequency field, is closer to the $N_1H$ proton.

This arrangement of $CH_2$ protons creates favourable conditions for intramolecular contact between the hydrogen atom $H_B$ and the carboxyl group attached to the $C_3$ carbon, resulting in the formation of |C-$H_B$|···O=C hydrogen bond. In addition, confirmation of the existence of the |C-H|···O hydrogen bond in compounds **2**–**4** comes from the deuteration rate of 2,6-$CH_2$ protons (Fig. 9). In the $D_2O$ solution of compound **4b**, the intensity of the $H_A$ resonance signal of the more strongly shielded protons decreases faster than that of the unshielded proton $H_B$. The reason for this is that the hydrogen-bonded protons are generally less affected by intermolecular H/D exchange. This fact confirms that a hydrogen bond is formed between proton $H_B$ of the methylene group and the carboxyl group.

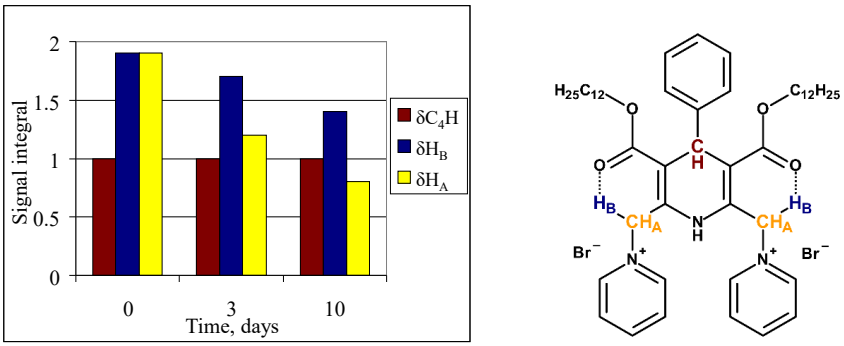


Fig. 9. $^1$H NMR spectral data for $D_2O$ solution of 1,4-DHP derivative **4b** in time at 25 °C.

As mentioned above, for some 1,4-DHP derivatives, the intramolecular hydrogen bond of |C-H|···O=C type is the reason for a large difference in the $^1$H NMR chemical shifts of the non-equivalent protons. It should be noted that in the $^1$H NMR spectra of almost all the compounds studied (**2**–**6**), $^1$H resonance signals of the protons of the methylene groups are characterized by an unusual temperature dependence (Fig. 10). The reversible evolution of the AB-type signals of the compounds studied when the temperature of the solution changes, excludes the possibility of viewing the process as a normal exchange because for these compounds there is no observable broadening of the resonance signals before their coalescence that is typical for the exchange processes. In addition, the chemical shifts of the $H_A$ and $H_B$ protons change.

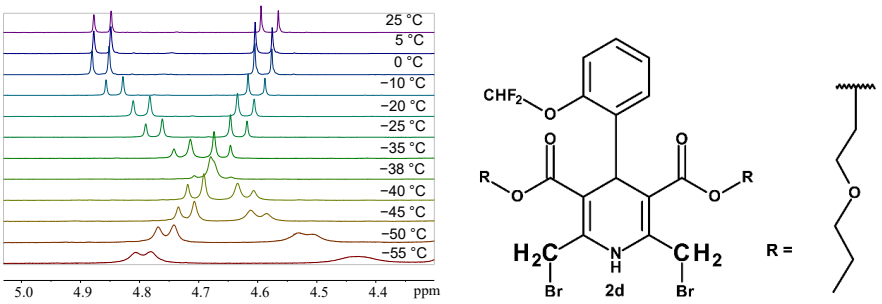


Fig. 10. Temperature dependence of the $^1$H NMR signals of the $C_{2,6}$-$CH_2$ methylene groups protons of compound **2d**. Spectra were recorded in $CDCl_3$ solution.

According to the literature data [31], the compounds studied have a very flexible 1,4-DHP cycle in which a rapid change of bath-chair conformations takes place, which is practically impossible to stop even at low temperatures. Therefore, the inversion of the 1,4-DHP cycle cannot be the main cause of the non-equivalence of the methylene group protons. For monocyclic compounds **2**, the possibility of hindered rotation around bonds $C_{2,6}$-$CH_2$ and $C_{3,5}$-COO should be considered during the determination of the most likely spatial structures. One of the ways to identify possible conformers in molecules with multiple degrees of freedom is to calculate the potential energy surfaces (PES) of the possible conformers.

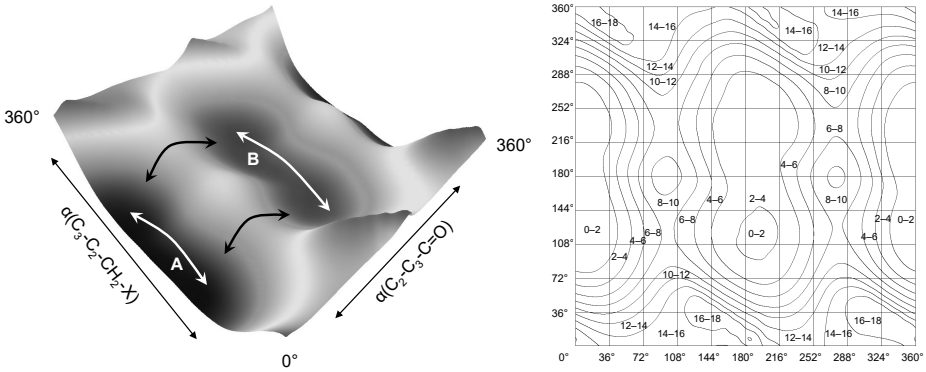


Fig. 11. PES and its projection for compound **2f**. X axis – angle for rotation around the $C_3$-$CO_2$ bond, Y axis – for rotation around the $C_2$-$CH_2$ bond, energy unit – kcal/mol. Transition barriers between conformations are shown by arrows.

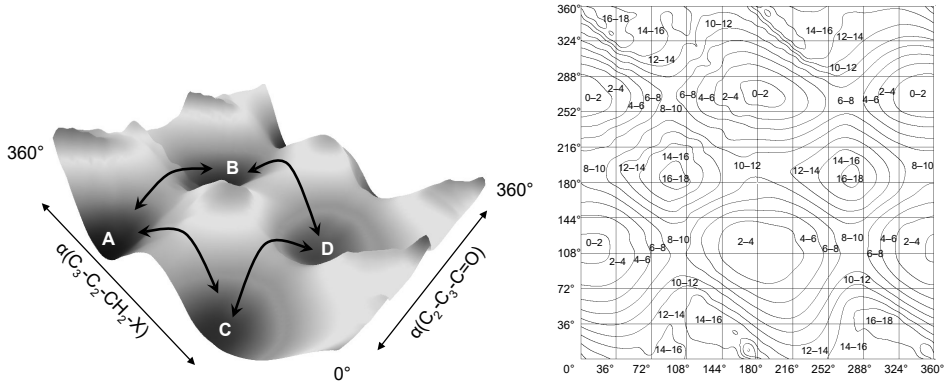


Fig. 12. PES and its projection for compound **2b**. X axis – angle for rotation around the $C_3$-$CO_2$ bond, Y axis – for rotation around the $C_2$-$CH_2$ bond, energy unit – kcal/mol. Transition barriers between conformations are shown by arrows.

For compounds **2f** and **2b**, scanning was performed by rotating around the $C_3$-$CO_2$ and $C_2$-$CH_2$ bonds (changing the dihedral angles $C_2$-$C_3$-C=O and $C_3$-$C_2$-$CH_2$-X by constraining these angles with the step of 10 angular degrees) and optimizing the entire remaining part of the molecule. Using the density-functional theory method (Jaguar 8.0 software package [22], level of theory DFT B3LYP/6-31G*), PES calculations were performed for structures that are model compounds for derivatives **2b** and **2f** (to speed up the calculations, bromine atoms were replaced by chlorine atoms). The three-dimensional PESs obtained in the calculations and their projections are shown in Figs. 11 and 12, with the energy of the optimal conformation taken as

a reference point. For compound **2f**, which has a substituted $N_1$, only two broad minima **A** and **B** can be identified in the PES for rotation around the $C_{2,6}$-$CH_2$ bond. For compound **2b**, four energy minima (**A**, **B**, **C** and **D**) are localized.

The energy barriers for the internal rotation of the carboxyl group around the $C_{3,5}$-$COOR_1$ bond (when the dihedral angle $C_2$-$C_3$-C=O is 80–110° and 260–290°) for compounds **2f** and **2b** are approximately the same, 8–10 kcal/mol. For compound **2f**, there are two very different barriers for rotation around the $C_{2,6}$-$CH_2$ bond (one ~0.4–2.2 kcal/mol, the other ~16–18 kcal/mol). The second barrier is 0.4 kcal/mol for **A** conformations and ~2.2 kcal/mol for **B** conformations. Such a small barrier results in the $C_{2,6}$-$CH_2$ methylene group protons of compound **2f** swing in two broad energy minima on the energy surface (dihedral angle $C_3$-$C_2$-$CH_2$-X range 70–300°). Decreasing the temperature does not slow this process down enough to register the signals of individual conformers. Therefore, the AB-protons of the methylene group of the studied compounds **2f** and **2b** are represented by conformer-averaged resonance signals, whose population is temperature dependent.

Their shielding can reach a point where they become isochronic with the same chemical shifts. For compound **2b**, in addition to the observed rotational barrier around the $C_{2,6}$-$CH_2$ bond, which is the same as for compound **2f** and corresponds to 16–18 kcal/mol (dihedral angle $C_3$-$C_2$-$CH_2$-X 100-120°), there is another 8–12 kcal/mol high barrier; dihedral angle $C_3$-$C_2$-$CH_2$-X 300–320°. A significant barrier to rotation around the $C_{2,6}$-$CH_2$ bond in the 1,4-DHP derivative **2b** allows the recording of proton resonance signals of the methylene groups of individual conformers in a low-temperature NMR experiment (Fig. 13).

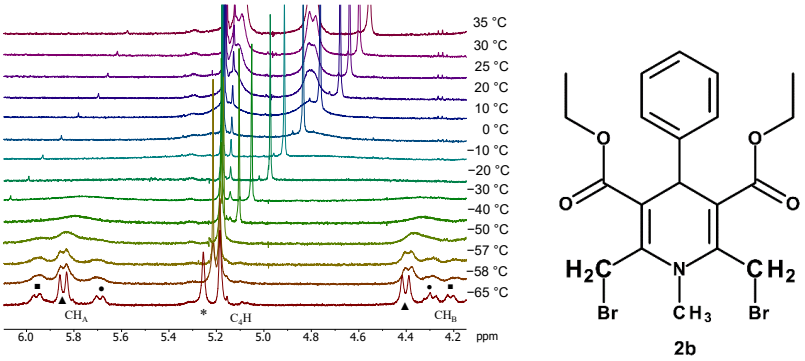


Fig. 13. Temperature dependence of the $^1$H NMR signals of compound **2b** $C_{2,6}$-$CH_2$ methylene group protons in tetrahydrofuran-$D_8$ solution (■, ▲, ● – symbols of AB spin systems, * – impurity of labile protons in the solvent) [16].

By evaluating the temperature dependence of the $^1$H NMR spectra of compound **2b**, it is possible to approximately estimate the coalescence temperature ($T_C$) of the proton resonance signals of the methylene group in $CDCl_3$ (−25 °C) and THF (−15 °C) solutions. Using Eyring's equation [32], it is possible to approximate the free activation energies for the conformational transitions (**A** ↔ **B**, **A** ↔ **C**, **C** ↔ **D** and **B** ↔ **D**) at the respective $T_C$ THF (~11.3 kcal/mol) and $CDCl_3$ (~10.7 kcal/mol) values. The obtained energy barrier values are only slightly higher than their calculated values. During these transitions, the conformation of only one part of the mobile molecule changes: halogen or carboxyl groups. The existence of at least three conformers probably indicates a significant population of asymmetric conformers of the substituents at the $C_{2,6}$ positions at low temperatures. Simultaneous change of orientations of

substituents at carbon atoms $C_{3,5}$ and $C_{2,6}$ (transitions **A** ↔ **D** and **B** ↔ **C**) seems unlikely because the energy barriers of this type of transitions are of the order of 16–18 kcal/mol.

### 2.2. 1,4-DHP derivatives with intramolecular hydrogen bonds of the type |N-H|···O=C

X-ray analysis of the structures of 1,4-DHP 3,5-mono- and 3,5-dicarboxylates as well as quantum chemical calculations [33] show that the carbonyl group is in *s-cis*, *s-cis* conformation relative to the $C_3$=$C_2$ or $C_6$=$C_5$ double bond. This is unusual, as it is well known that the *s-trans* orientation is preferred for better conjugation, as well as the *s-trans* orientation is also more stable [34]. The reason for the peculiar *s-cis* structure of the fragment C=C-C=O is unclear. However, in the case of 1,4-DHP derivatives, it has been hypothesized that the *s-cis* orientation is supported by a weak intramolecular hydrogen bond |C-H|···O=C interaction. This kind of interaction is also possible for compounds **1**, **5** and **6** (Table 3).

Table 3

1,4-DHP derivatives **1**, **5** and **6**

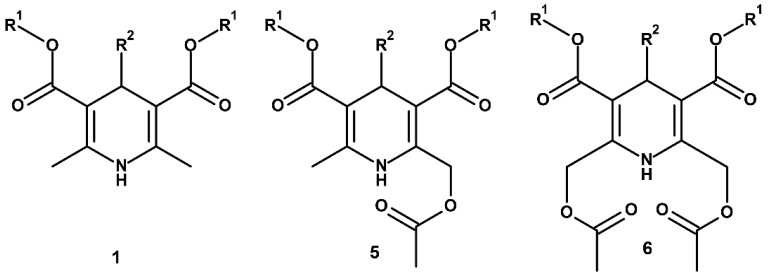

| No. | Comp. | $R^1$ | $R^2$ |
|---|---|---|---|
| 1. | **1a** | $CH_2CH_3$ | $CH_3$ |
| 2. | **1b** | $CH_2CH_3$ | Ph |
| 3. | **1c** | $(CH_2)_2OC_3H_7$-*n* | $PhOCHF_2$-*o* |
| 4. | **5a** | $CH_2CH_3$ | $CH_3$ |
| 5. | **5b** | $CH_3$ | $CH_3$ |
| 6. | **5c** | $CH_2CH_3$ | Ph |
| 7. | **5d** | $(CH_2)_2OC_3H_7$-*n* | $PhOCHF_2$-*o* |
| 8. | **5e** | $CH_2CH_3$ | Ph-F-*o* |
| 9. | **5f** | $CH_2CH_3$ | Ph-$NO_2$-*m* |
| 10. | **6a** | $CH_2CH_3$ | $CH_3$ |
| 11. | **6b** | $CH_2CH_3$ | Ph |
| 12. | **6c** | $(CH_2)_2OC_3H_7$-*n* | $PhOCHF_2$-*o* |

The signals of the methylene groups of the alkoxycarbonyl chains at positions 3 and 5 of the 1,4-DHP cycle in compounds **5** and **6** show splitting because the $C_4$ carbon atom is a chiral (or prochiral) centre. Other signals in the $^1$H NMR spectra correspond to the nature of aromatic or aliphatic hydrogen atoms. In the $^1$H NMR spectra of compounds **5** and **6**, two protons of the methylene groups at the $C_2$ and $C_6$ substituents are also diastereotopic, and the signals can be described as AB systems in the range of 5.24–5.44 ppm. Nonequivalence of these protons is characterized by a difference in the $^1$H chemical shifts ($\delta(H_A)$-$\delta(H_B)$), which can be influenced by factors such as the conformation of the 1,4-DHP cycle, anisotropic effect of the substituents, hindered rotation of the substituents attached to the $C_2$ and $C_6$ carbon atoms, and the intramolecular hydrogen bond of the type |C-H|···O. The geminal spin-spin coupling constants $^2J(H_A, H_B)$ values increase slightly from 14.8 Hz (**5**) to 15.2 Hz (**6**). For compounds **5**,

depending on the substituents at the $C_4$ carbon atom, the observed difference in the chemical shifts of the AB-protons of the methylene groups is within 0.04–0.13 ppm.

With the temperature changes, the chemical shift of the $H_A$ proton for compounds **5** and **6** change linearly with the same coefficient as the chemical shift of the methyl group protons at $C_2$ and $C_6$ for compounds **1**. Thus, the proton $H_A$ should be as accessible to the solvent (chloroform) as in compound **1**. At the same time, the signal of the proton $H_B$ changes nonlinearly and the shape of the curve is close to a negative parabola (Fig. 14). The nonlinear dependence of the value $\delta(H_B)/T$ indicates that the $H_B$ proton is involved in the formation of the weak intramolecular hydrogen bond of type |C-H|···O=C.

Broad NH proton signals are observed in the $^1$H NMR spectra at 5.54–5.73 ppm. (**1**), 6.48–6.67 ppm. (**5**) and 7.55–7.77 ppm. (**6**). The downfield shift of the $N_1H$ proton signal for compounds **1** → **5** → **6**, respectively, may reflect the formation of an intramolecular $|N_1\text{-}H|\cdots O$ hydrogen bond between the $N_1H$ proton and the $COOCH_3$ oxygen atoms at the $C_2$ and $C_6$ carbon atoms of compounds **5** and **6** [35].

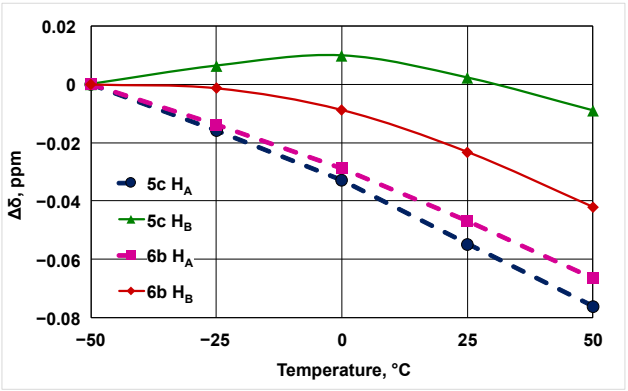


Fig. 14. Temperature dependence of the $C_{2,6}$-$CH_2$ methylene protons $^1$H chemical shifts for compounds **5c** and **6b** in $CDCl_3$ solutions. The solid and dashed lines represent the values for the $H_A$ and $H_B$ protons, respectively. The chemical shifts of each proton at −50 °C are taken as the zero point. **5c** $H_A$ (●), **5c** $H_B$ (▲), **6b** $H_A$ (■) and **6b** $H_B$ (◆).

The temperature coefficient ($\Delta\delta/\Delta T$) of the proton $N_1H$ NMR signal is commonly used to determine the presence of an intramolecular hydrogen bond [35]. The breaking of hydrogen bonds caused by an increase of the temperature moves the resonance signal of the $N_1H$ proton upfield. The temperature coefficients greater than −4.5 ppb/K are very indicative of intramolecular hydrogen bonds. The temperature coefficients of the $N_1H$ proton resonance signals for compounds **1**, **5** and **6** were obtained by recording $^1$H NMR spectra in $CDCl_3$ solutions in the temperature range −50...+50 °C. The obtained values are between −2.5 and −10.4 ppb/K. The $\Delta\delta/\Delta T$ value of the NH proton of compound **6** is greater than −4.5 ppb/K (about −3 ppb/K), which indicates the involvement of this proton in intramolecular hydrogen bond formation. Compounds **6**, which have two acetoxymethyl groups as substituents and therefore can form two hydrogen bonds, have lower $\Delta\delta/\Delta T$ values than compounds **5** (about −3.6 ppb/K). A consequence of this could be a weaker |N-H|···O=C hydrogen bond for compounds **5** compared to **6**.

The absolute values of the measured spin-spin coupling constants $^1J(^{15}N,^1H)$ are in the range 92–96 Hz and increase slightly for the compounds studied in the order **1** → **5** → **6**, indicating

that the hydrogen is stably bound to the nitrogen atom and that there is a small intermolecular exchange, which contradicts the literature data [36], because the increase of positive charge or deshielding of the $N_1$-H proton should decrease the absolute value of $^1J(^{15}N,^1H)$. However, if the nitrogen of the proton donor is $sp^2$ hybridized, the changes in $^1J(^{15}N,^1H)$ values are quadratically related to the length of the corresponding $N_1$-H distance: the shorter the $N_1$-H bond, the larger $^1J(^{15}N,^1H)$ value [37]. This could indicate a slight decrease in the $N_1$-H distance for compounds in the order **1** → **5** → **6**.

According to the literature data [38], when NH takes part in the formation of the |N-H|···X hydrogen bond, the spin-spin coupling constant $^1J(^{15}N,^1H)$ is mainly affected by two factors – the electrostatic effect and the (X)→(N-H) charge transfer. It is known that the first factor causes an increase in the absolute value of $^1J(^{15}N,^1H)$, while the second causes a decrease in the absolute value of $^1J(^{15}N,^1H)$. The effects of these two factors on the IR stretching frequency of the $N_1$-H bond are opposite to each other, so the charge transfer interactions correspond to a red shift, while the electrostatic effect causes a blue shift. In general, hydrogen bonds lead to an elongation of the X-H covalent bond and its stretching vibration $\nu$(XH) shifts to the lower wavenumbers (red shift) [35], [39]. The shift of $\nu$(NH) to the higher wavenumbers in the case of hydrogen bonding is probably related to the decrease of the $N_1$-H distance (blue shift). This type of effect has been reported for the C-H and N-H bonds [40].

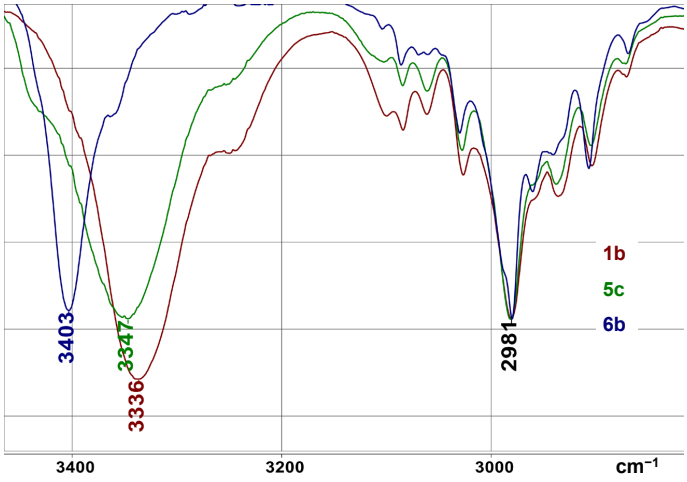


Fig. 15. Stretching frequencies of the N-H and C-H bonds in the IR spectra for **1b**, **5c** and **6b**.

The IR spectral data for compounds **1a-c** (without hydrogen bonds) are characterised by the stretching $\nu$(NH) bands in the range 3344–3336 $cm^{-1}$. The NH groups which are involved in one hydrogen bond formation in compounds **5a-d** show the N-H stretching vibration in the interval 3347–3348 $cm^{-1}$, while the NH groups engaged in two hydrogen bonds in compounds **6a-c** display the $\nu$(NH) bands in the interval 3363–3437 $cm^{-1}$ (Fig. 15). The observed $\nu$(NH) band moves up to 11 $cm^{-1}$ on going from **1b** to **5c** and up to 67 $cm^{-1}$ on going from **1b** to **6b**. The frequencies of the NH stretching band ($\nu$(NH)) and the values of the constants $^1J(^{15}N,^1H)$ for compounds **1**, **5** and **6** indicate that the changes in both these parameters ($\nu$(NH) and $^1J(^{15}N,^1H)$) can partially be caused by the same reason – the differences in the length of the $N_1$-H bond [41].

The $^{1}$H-$^{15}$N HMQC spectra with the value of the N-H direct coupling constant ($^{1}J(^{15}N,^{1}H) = 95$ Hz) have been used to measure the $^{15}$N chemical shifts [33], [42]. The $^{15}$N resonance signals appear in three distinct regions: 134.53–134.01 ppm (**1**), 123.31–124.42 ppm (**5**) and 114.18–115.58 ppm (**6**).

The downfield shift of the $N_1H$ proton signal ($N_1H$ deshielding) is accompanied by the upfield shift of the $^{15}$N resonance signals ($N_1$ shielding) in the order for compounds **1** → **5** → **6** (Fig. 16). This is surprising, since the shielding of the NH proton is usually accompanied by the shielding of the adjacent nitrogen atom [43]. Usually, the NH bond elongates on hydrogen bond formation [44]. According to the literature data [45], the observed $^{15}$N chemical shifts of the amide nitrogens move upfield, with the shortening of the |N-H| bond in the |N-H|···O=C hydrogen bond. Thus, the reverse dependence of $\delta(^{15}N)/\delta(^{1}H)$ in the sequence **1** → **5** → **6** probably indicates the shortening of the N-H bond, but the significant upfield shift of the $^{15}$N resonance signal in the same sequence of the compounds (**1** → **5** → **6**) cannot be quantitatively explained.

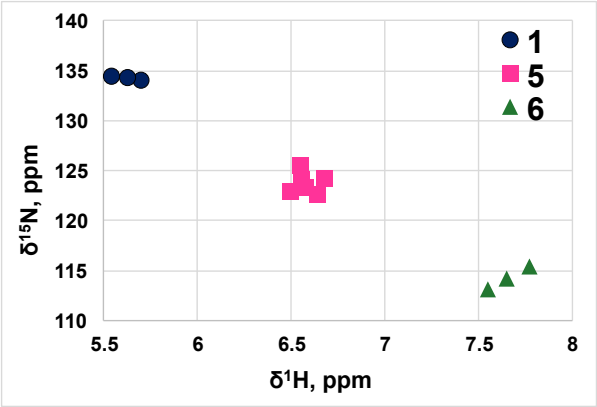


Fig. 16. Relationship between $^{15}$N and $^{1}$H chemical shifts 1(●), 5(■) and 6(▲).

The $\delta(^{1}H)$ downfield shift and $\delta(^{15}N)$ upfield shift for the compounds in the sequence **1** → **5** → **6** can be partially induced by the shortening of the N-H bond. This is confirmed by the increase in the absolute value of $^{1}J(^{15}N,^{1}H)$ in the sequence **1** → **5** → **6**. A possible explanation for the diamagnetic shift of heavy nuclei may be the steric perturbations due to the nearby electron cloud. In this case, this could be due to the spatial affinity between the acetoxy substituent and the $^{15}$N nucleus. According to the literature data [46], such an effect could shift the $^{15}$N resonance signal up to 10 ppm to higher fields.

The secondary deuterium-proton isotope effects (IE) ($^{n}\Delta^{13}C(H/D)$) are very good tool to study intramolecular hydrogen bonds [47]. All the effects from proton substitution to deuterium can be quickly detected by $^{13}$C NMR spectroscopy, as the $^{n}\Delta^{13}C(H/D)$ can be transmitted not only through chemical bonds, but also through space. In compounds **1**, **5**, **6**, the replacement of the proton attached to the nitrogen atom by deuterium produces only the intrinsic IE, since the $^{1}J(^{15}N,^{1}H)$ values of approximately ~92–96 Hz, allow to neglect any equilibrium processes. The intrinsic IE have a vibrational origin and are related to the anharmonicity of the |N-H|···X bond potential curve. Hydrogen bonding increases this anharmonicity. The changes in NMR $^{13}$C shift values are caused by the shortening of the N-H/D bond upon deuteration [48].

The values of IE ($^{n}\Delta^{13}C(H/D) = \delta(^{13}C(N_1H)) - \delta(^{13}C(N_1D))$) were measured in the $^{13}C$ spectra of partially deuterated samples, where the signals of both isomers could be easily identified by their relative intensities (Table 4). All measured IE for compounds **1**, **5** and **6** are positive. The effect of substituents on IE values is mainly characterized by two factors: the hydrogen bonding and the transfer of the electronic effects of substituents [49]. The N(H/D) isotope effects on the acetoxymethyl carbonyl $^{13}C$ atoms have been registered (Table 4). For compound **5**, where the $N_1H$ proton is involved in one hydrogen bond, the $^{5}\Delta^{13}C_{COO}$ H/D values are in the range 3–5 ppb. At the same time, the $^{5}\Delta^{13}C_{COO}$ H/D IE values for the carbons of the carboxyl group for compounds **6** are 3–5 times higher (~15–18 ppb) than for compounds **5**.

Analysis of the influence of H/D substitution on the $^{13}C$ carbon atom NMR spectra of the 1,4-DHP cycle, shows that the changes in the sequence of compounds **1** → **5** → **6** are rather small. This corresponds to an equally small change in the chemical shifts of the $^{13}C$ spectra. Interestingly, the effect of H/D IE on the $C_{2,6}$-$^{13}CH_3$ atom in the methyl group, which is separated from the $N_1H$ proton by three bonds (~81–84 ppb), is similar because of IE on the $^{13}C_{2,6}$ carbon is separated by only two bonds (~80–96 ppb). At the same time, the IE values for $^{13}C_{3,5}$ atoms are much smaller (~41–59 ppb). The $^{13}C$ isotope shifts for methyl groups at positions 2 and 6 of the 1,4-DHP cycle in compounds **1** and **5** are significantly larger than for the methylene groups at the same carbon atoms in compounds **5** and **6**.

Table 4

H/D IEs on $^{13}C$ nuclei (ppb) in compounds **1, 5** and **6**

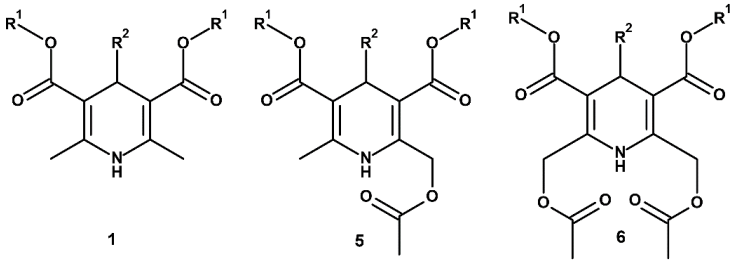


| No. | Comp. | $R^1$ | $R^2$ | COO···H | $C_6$ | $C_2$ | $C_5$ | $C_3$ | $C_6$-$CH_3$ | $C_2$-$CH_2$ |
|---|---|---|---|---|---|---|---|---|---|---|
| 1. | **1a** | $CH_2CH_3$ | $CH_3$ | - | 85 | 85 | 50 | 50 | 81 | - |
| 2. | **1b** | $CH_2CH_3$ | Ph | - | 84 | 84 | 51 | 51 | 82 | - |
| 3. | **1c** | $(CH_2)_2OC_3H_7$-*n* | $PhOCHF_2$-*o* | - | 90 | 90 | 47 | 47 | 84 | - |
| 4. | **5a** | $CH_2CH_3$ | $CH_3$ | - | 86 | 78 | 59 | 44 | 84 | 37 |
| 5. | **5b** | $CH_3$ | $CH_3$ | - | 88 | 79 | 59 | 45 | 84 | 37 |
| 6. | **5c** | $CH_2CH_3$ | Ph | 3 | 87 | 80 | 59 | 42 | 84 | 36 |
| 7. | **5d** | $(CH_2)_2OC_3H_7$-*n* | $PhOCHF_2$-*o* | 5 | 96 | 88 | 58 | 41 | 84 | 36 |
| 8. | **5e** | $CH_2CH_3$ | Ph-F-*o* | 5 | 94 | 87 | 58 | 41 | 84 | 35 |
| 9. | **5f** | $CH_2CH_3$ | Ph-$NO_2$-*m* | 4 | 91 | 85 | 57 | 43 | 84 | 37 |
| 10. | **6a** | $CH_2CH_3$ | $CH_3$ | 15 | 82 | 82 | 56 | 56 | - | 32 |
| 11. | **6b** | $CH_2CH_3$ | Ph | 18 | 85 | 85 | 55 | 55 | - | 33 |
| 12. | **6c** | $(CH_2)_2OC_3H_7$-*n* | $PhOCHF_2$-*o* | 18 | 91 | 91 | 53 | 53 | - | 34 |

The quantum chemical calculations using the Gaussian 09 (D.01.) software package [50] were carried out. Calculations performed at the theoretical level DFT B3LYP/6–311G++(d,p) show that the **5** $N_1H$ proton with the oxygen of the alkoxy group could preferably form a five-membered H-chelate type cycle. Two seven-membered H-chelate cycles of compounds **6** with C=O oxygens in the substituents at positions 2 and 6 of 1,4-DHP cycle are formed. Different

types of |N-H|···O bonds in **5** and **6** may be the reason for the increase in the values of the secondary ($^6\Delta^{13}$C(NH/D)) isotopic shifts in the $^{13}$C NMR spectrum on the carboxyl group carbon of the substituents at positions 2 and 6 upon shifting from **5** to **6**. The IEs of NH/D substitution through six chemical bonds on the $^{13}$C chemical shifts of the carboxyl carbons at positions 2 and 6 ($^6\Delta^{13}$C(NH/D)) (**6**) are larger than the isotope effects through four chemical bonds ($^4\Delta^{13}$C(NH/D)) (**5**); this proves that the |N-H|···O hydrogen bond in the seven-membered H-chelate cycle formed by the C=O group is stronger than the bond in the five-membered H-chelate cycle formed by the alkoxy group.

## 3. Cationic lipids based on 1,4-DHP derivatives and their binding to mononucleotides

The study was conducted to determine the binding ability of mononucleotides (as prodrug models) to cationic amphiphilic lipid-like 1,4-DHP derivatives **4** (Table 5 and Fig. 17). The compounds of this type show the ability to self-aggregate and form vesicles in aqueous solutions [17], [51], [52]. Among the two cationic substituents containing cationic amphiphiles, the highest transfection activity was shown by 1,4-DHP derivative **4b** with two C12 alkyl chains in the ester groups. The introduction of methyl substituent at the $N_1$ atom of the 1,4-DHP cycle, as well as the shortening or elongation of the alkyl chains (at positions 3 and 5) leads to a decrease in the transfection activity or even to its complete loss [19].

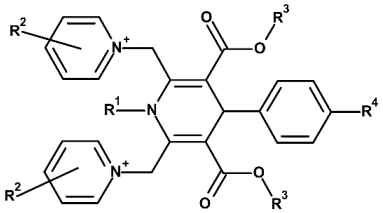


Fig. 17. The structures of studied compounds **4**.

Table 5

Studied cationic amphiphilic 1,4-DHP derivatives **4**

| No. | Comp. | $R^1$ | $R^2$ | $R^3$ | $R^4$ |
|---|---|---|---|---|---|
| 1. | **4b** | H | H | $C_{12}H_{25}$ | H |
| 2. | **4d** | H | H | $C_{16}H_{33}$ | H |
| 3. | **4e** | $CH_3$ | H | $C_{12}H_{25}$ | H |
| 4. | **4f** | H | *p*-$CH_3$ | $C_{12}H_{25}$ | H |
| 5. | **4g** | H | 3,5-$CH_3$ | $C_{12}H_{25}$ | H |
| 6. | **4h** | H | *p*-$N(CH_3)_2$ | $C_{12}H_{25}$ | H |
| 7. | **4i**[a] | H | H | $C_{12}H_{24}$-$CF_3$ | H |
| 8. | **4j** | H | H | $C_{12}H_{25}$ | $CF_3$ |

*a* perchlorates, all the others – bromides.

The mechanism of complexation between DNA or RNA and 1,4-DHP **4** is not completely clear, but the association depends on the nucleic acid-forming mononucleotides [53]. It is therefore reasonable to compare the ability of 5'-mononucleotides (Fig. 18) to bind with the cationic 1,4-DHP type amphiphiles (**4**). This would be important to efficiently predict, search and synthesize new cationic amphiphiles with optimal structures for effective drug delivery and

gene transfection. To determine the binding energy, the structure of complexes of four RNA 5'-mononucleotides with 1,4-DHP derivatives **4** was studied using isothermal titration calorimetry (ITC) and NMR spectroscopy. At the beginning it was planned to evaluate the binding of the most active compound **4b** to 5'-mononucleotides and to analyse how the variation of the substituents in the structure of **4** affects their complexation ability.

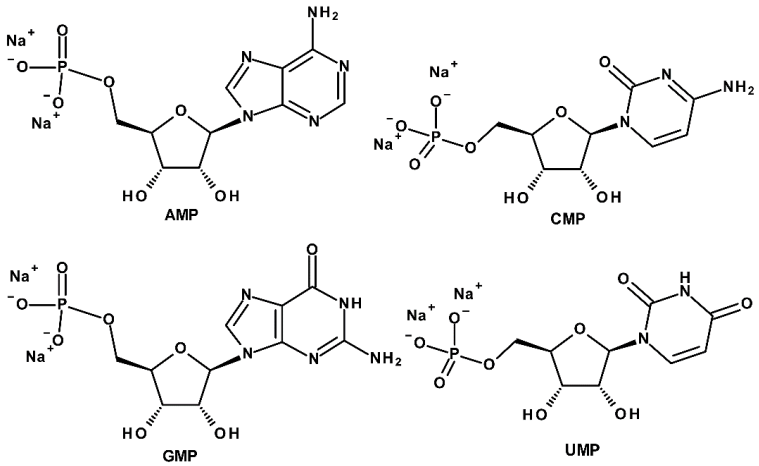


Fig. 18. RNA 5'-mononucleotides.

### 3.1. Studies of self-assembly of cationic amphiphilic lipid-like 1,4-DHP derivatives

The ITC method is very important for the determination of various thermodynamic parameters of binding and is often used for the determination of the critical vesicle concentration (CVC) [54]. The ITC data (Fig. 19) are well described by the Boltzmann sigmoid (Equation (1)).

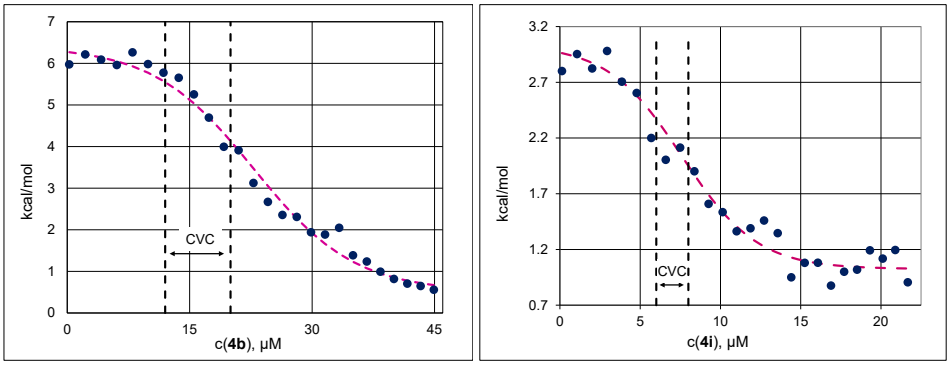


Fig. 19. The ITC data for determination of **4b** and **4i** CVC values (the cationic lipid concentration in the syringe for **4b** – 270 μM and for **4i** – 130 μM). Pink colour dashed lines are fitted according to Equation (1). The x-scale corresponds to the concentration of **4** in the cell. Black vertical dashed lines correspond to the CVC region.

$$Q^{\text{deves}} = \frac{A_1 - A_2}{1+e^{\frac{c_{\text{det}} - \text{CVC}}{\Delta}}} + A_2, \qquad (1)$$

where $c_{\text{det}}$ is the concentration of the cationic amphiphilic lipid-like 1,4-DHP derivative (detergent) in the iTC200 titration cell, Δ is the width of the transition region, $Q^{\text{deves}}$ is the heat

of vesicle dilution (devesiculation), $A_1$ and $A_2$ are the initial and the final values. The $Q^{deves}$ was normalised using the concentration in the titration syringe and the CVC value.

At the beginning of the titration, the concentration of 1,4-DHP derivatives **4** in the cell was below the CVC. The titration curve (Fig. 19) shows that the dissociation of the vesicles is an endothermic process. After reaching the CVC, the dissociation energy decreased to almost zero, as the vesicles were no longer dissociating and only the thermal effect of dilution was observed. The CVC values and the thermodynamic data for compounds **4** are given in the Table 6. The driving force for self-aggregation is a hydrophobic effect, which depends on the lipophilicity of the molecules. It is well known that the CVC decreases with increasing of lipophilicity of the surfactants [55]. The CVC values of the 1,4-DHP derivatives **4** obtained with ITC are relatively low. Compounds **4g**, **4h**, **4i** and **4j** are characterized by lower CVC values due to their higher lipophilicity [56]. To evaluate the lipophilicity of derivatives **4**, the values of the octanol/water partition coefficient (logP) were calculated (Table 6). The CVC and logP values of 1,4-DHP derivatives **4** correlate, showing an increase in lipophilicity.

Table 6

LogP values, CVC and thermodynamic parameters of 1,4-DHP derivatives **4**

| Comp. | logP | CVC, μM | $\Delta G^{\circ,ves}$, kcal/mol | $\Delta H^{\circ,ves}$, kcal/mol | $-T\Delta S^{\circ,ves}$, kcal/mol |
|---|---|---|---|---|---|
| **4b** | 15.2 | 16 ± 4 | −8.9 | −6.6 | −2.3 |
| **4e** | 15.0 | 17 ± 2 | −8.9 | −7.6 | −1.3 |
| **4f** | 15.9 | 17 ± 3 | −8.9 | −6.7 | −2.2 |
| **4g** | 16.5 | 10 ± 2 | −9.2 | −5.3 | −3.9 |
| **4h** | 16.0 | 11 ± 2 | −9.1 | −7.2 | −1.9 |
| **4i** | 17.7 | 7 ± 1 | −9.4 | −2.2 | −7.2 |
| **4j** | 16.2 | 10 ± 2 | −9.2 | −3.1 | −6.1 |

During vesiculation, water is released from the inner parts of the vesicles (as amphiphilic molecules have a hydrophobic part), and the water structure becomes disordered, resulting in an increase in the entropy [57]. From the results given in Table 6, it can be generalized that the vesiculation of compounds **4** at 25 °C is an exothermic process. The Gibbs free energy ($\Delta G^{\circ,ves}$) as well as the enthalpy ($\Delta H^{\circ,ves}$) have a negative value, while the entropy ($S^{\circ,ves}$) has a positive value.

### 3.2. Binding of RNA 5'-mononucleotides to 1,4-DHP derivatives, $^1$H NMR titration

The formation of complexes occurs in a process of association and dissociation of components. The stability of the complex is determined by its lifetime. $^1$H NMR titration experiments were performed to characterize 1,4-DHP derivative **4** and 5'-mononucleotide complexes. $^1$H NMR titration experiments are informative, as they allow the thermodynamic data of the system to be determined. In the case of the mononucleotides **CMP** and **UMP**, the exchange process with 4 was fast (on the $^1$H NMR time scale) and the average NMR proton signals of both free and bound molecules were recorded (Equation (2)):

$$\delta_{observed} = Y_{free} \times \delta_{free} + Y_{bound} \times \delta_{bound} \quad (2)$$

The dissociation constants ($K_D$) of the complexes of compounds **4** with mononucleotides **CMP** and **UMP** were calculated using Equation (3) by recording the changes of the $^1$H proton signals at different concentration ratios of **4** to mononucleotide [58]. Two unknowns – the

dissociation constant ($K_D$) and the chemical shift ($\delta_{bound}$) of bound RNA 5'-mononucleotides and 1,4-DHP **4** were estimated using non-linear fitting:

$$\delta_{observed} = (\delta_{free} - \delta_{bound}) \frac{K_D + C_H + C_G - \sqrt{(K_D + C_H + C_G)^2 - 4 \times C_H \times C_G}}{2} + \delta_{free}, \quad (3)$$

where, $C_H$ and $C_G$ are the concentrations of the host and guest, respectively.

The dissociation constants for host (mononucleotide) – guest (1,4-DHP derivative) interactions were calculated from the titration curves of the H1' proton signal of 5'-mononucleotides upon the addition of an increasing amounts of **4** to the solution. The dissociation constants ($K_D$) of all host/guest systems are of the same order (Table 7). The smaller values of the constants indicate stronger binding. The data show that the most energetically favourable complexes are formed by **4i** with **CMP** and **UMP**.

Table 7

The dissociation constants $K_D$ (nM) for **4** and mononucleotide complexes

| 5'-mononucleotide | **4b** | **4d** | **4e** | **4f** | **4g** | **4h** | **4i** | **4j** | **4b**/DPPC |
|---|---|---|---|---|---|---|---|---|---|
| **CMP** | 23 | 98 | 33 | 16 | 26 | 16 | 4 | 32 | 31 |
| **UMP** | 26 | 92 | 28 | 24 | 22 | 21 | 10 | 56 | 60 |

The substituents in the pyridinium ring (**4f**, **4g** and **4h**) slightly modify the stability of the complexes of the respective compounds with mononucleotides. On the other hand, the N-$CH_3$ substituted 1,4-DHP derivative **4e**, as well as the compound **4j** with p-$CF_3$–phenyl substituent at position 4 of the 1,4-DHP cycle and the vesicles composed of the mixture of **4b** with dipalmitoylphosphatidylcholine (DPPC) (1 : 3), showed higher values of the dissociation constants than pure **4b**. The 1,4-DHP derivative **4d** with C16 alkyl chains in the ester groups shows weaker binding ability.

For **AMP** and **GMP**, the exchange rates at 25 °C were in the medium range of the NMR time scale, and it was not possible to estimate $K_D$ values due to the significantly broadened signals (at concentration ratios between 0.3 and 1.2). **AMP** showed less broadened signals, but the chemical shift measured at the current temperature was not suitable for $K_D$ determination.

Thus, the ability of 1,4-DHP vesicles to form complexes depends on the length of the alkyl chains of the esters at positions 3 and 5 of the 1,4-DHP cycle. Derivative **4i** with long alkyl chains, where the terminal $CH_3$ is replaced by $CF_3$ groups, shows a stronger binding ability to RNA 5'-mononucleotides. This improved binding could be explained by different chain dynamics due to the hydrophobic interaction of the fluorine atoms. This is reflected in lower CVC values for compound **4i** compared to the other studied 1,4-DHP derivatives. Different substituents at positions 2 and 6 of the 1,4-DHP cycle have only a minor effect on the binding ability of 1,4-DHP derivatives **4**. Modification of the phenyl substituent to *p*-CF3-phenyl- at position 4 of the 1,4-DHP cycle decreases its association with mononucleotides. The mixture formed by compound **4b** and DPPC (to form co-vesicles) reduces the ability of the vesicles to bind to 5'-mononucleotides when compared to the vesicles formed by **4b** only.

### 3.3. Complexation of RNA 5'-mononucleotides with 1,4-DHP derivatives, comparison of the data obtained from $^1$H NMR and ITC studies

In addition to $^1$H NMR titration, the dissociation constant was also determined using the ITC method. This method is also very popular for *in vitro* affinity/binding determinations

because it is fast, simple and direct [59]. It provides excellent insight into binding processes with greater accuracy compared to other methods [60]. On the other hand, the method is sensitive not only to molecular binding. It is also sensitive to various other processes in the titration cell (buffer mismatch, dilution, impurities, etc.), which greatly complicates the interpretation of the results obtained.

In all binding ITC titration experiments, the concentration of **4** in the titration cell after the second injection was higher than its CVC value (the concentration of **4** in the titration syringe was ~3.5 mM). To separate the reorganization energy of the vesicles from the binding energy, the reference titration experiments were performed (vesicles of **4** were injected into a cell filled with pure water) [61]. Usually, ITC titration experiments show as S-shaped curve (Fig. 20), from which thermodynamic parameters are calculated.

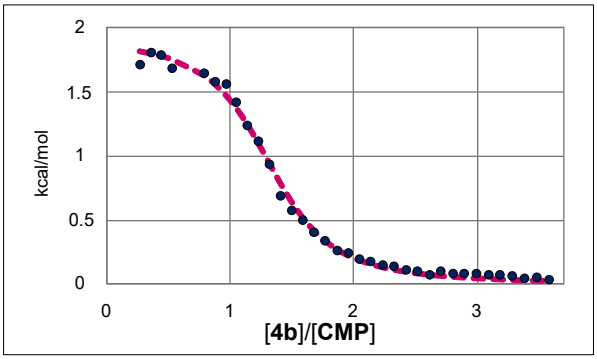


Fig. 20. ITC experimental data for **CMP** (cell) and **4b** (syringe), (the fitted values are represented by dotted lines).

The values of the dissociation constant $K_D$ and the thermodynamic parameters are given in Table 8. In addition to the $^1$H NMR spectroscopy methods, the thermodynamic parameters of the complexes were determined by ITC. The $K_D$ values determined by the ITC method are smaller than those obtained by $^1$H NMR titration. This is not surprising, since the changes in chemical shifts observed in $^1$H NMR titration experiments occur only when the corresponding proton is involved in complex-forming interactions (also the chemical shift does not always corresponds to complexation), in contrast to ITC measurements that record any binding (change in heat) regardless of the type of interaction [62]. Binding characteristics for complexes are shown by the contribution of the enthalpy ($\Delta H$) and the entropy ($-T\Delta S$) to the Gibbs free energy of binding ($\Delta G$). The opposite contributions of enthalpy and entropy result in a modest change in the Gibbs free energy ($\Delta G \approx -7$ kcal/mol). The negative entropy factors are mainly due to non-specific hydrophobic interactions and desolvation.

The values of the ΔG, ΔH and ΔS indicate that the binding processes are dominated by entropic interactions [63], which is in agreement with literature data on ammonium lipid vesicles [64]. Entropy of the hydrophobic interaction favours the binding of 1,4-DHP derivatives **4** and 5'-mononucleotides.

Table 8

The values of the $K_D$ and the thermodynamic parameters of titration of 5'-mononucleotide with **4b** determined by ITC and $^1$H NMR

| Mononucleotide | NMR | ITC | NMR | ITC | | |
|---|---|---|---|---|---|---|
| | $K_D$, nM | | $\Delta G$, kcal/mol | | $\Delta H$, kcal/mol | $\Delta S$, cal/(mol×K) |
| **AMP** | - | 10 ± 6 | - | −7.0 ± 0.4 | 2.1 ± 0.3 | 30 ± 1 |
| **CMP** | 23 ± 7 | 15 ± 6 | −6.3 ± 0.8 | −6.6 ± 0.3 | 5.1 ± 1.0 | 39 ± 1 |
| **UMP** | 26 ± 9 | 6 ± 2 | −6.3 ± 0.9 | −7.2 ± 0.2 | 4.6 ± 0.5 | 39 ± 3 |

The results of the **GMP** titration are different. Before the curve reaches a plateau (at the (3 : 2) ratio) two points of inflection were registered (with a difference of ~1 kcal/mol). The experiment was repeated several times and the same result was obtained each time – an increase in energy was observed before reaching the plateau. Perhaps this anomaly was caused by the **GMP** characteristic – a tendency to self-associate, which has also been mentioned in the literature [65]. It can be assumed that **GMP** interactions with 1,4-DHP derivatives **4** occur in two stages: at first, free **GMP** molecules bind to **4**; then, **GMP** clusters disperse – the amount of heat increases [66]. Therefore, using this method for **GMP** mononucleotide it was not possible to estimate the value of $K_D$ for the association with lipid-like 1,4-DHP derivatives.

### 3.4. Comparison of the formation of RNA 5'-mononucleotides complexes with the formation of complexes of some 1,4-DHP derivatives

The NMR T1ρ relaxation method allows the detection of ligand association due to the relaxation differences between small and large molecules [67]. 1,4-DHP vesicles can be considered as large molecules, while the mononucleotides can be considered as molecules. In the T1ρ experiment, the decrease in the intensity of the proton signals for mononucleotides is related to the shortening of the relaxation time and is proportional to the binding strength of "large molecules" and "small molecules". The change of integral intensities observed in the spectra of RNA 5'-mononucleotides when they bind to the vesicles formed by 1,4-DHP **4b** is shown in Table 9. The binding capacity of the mononucleotides decreases in the order: **CMP → UMP → AMP → GMP**.

Table 9

Decrease of RNA 5'-mononucleotide signal integral values (%) in $T_1\rho$ experiments

| Comp. | | H8 | H6, H1' | H6 | H5 | H1' | H2', H3' | H2' | H3' | H4' | H5' |
|---|---|---|---|---|---|---|---|---|---|---|---|
| **AMP** | **4b** | 23 | | | | 48 | | 23 | | 22 | 25 |
| | **4e** | 23 | | | | 64 | | 26 | | 26 | 34 |
| | **4i** | 50 | | | | 80 | | 58 | | 53 | 57 |
| **CMP** | **4b** | | | 97 | 94 | 89 | 96 | | | 94 | 98 |
| | **4e** | | | 49 | 32 | 38 | 56 | | | 56 | 69 |
| | **4i** | | | 86 | 75 | 65 | 84 | | | 80 | 97 |
| **GMP** | **4b** | 23 | | | | 40 | | | 18 | 19 | 19 |
| | **4e** | 14 | | | | 20 | | | 13 | 11 | 10 |
| | **4i** | 19 | | | | 24 | | | 16 | 14 | 16 |
| **UMP** | **4b** | | 36 | | 32 | | | 43 | 41 | 42 | 40 |
| | **4e** | | 8 | | 9 | | | 21 | 14 | 15 | 18 |
| | **4i** | | 76 | | 73 | | | 93 | 91 | 85 | 95 |

In comparison of nucleotide binding to the 1,4-DHP derivatives **4b**, **4e** and **4i** vesicles, average values of the $^1$H integral intensities show a decrease in the order of **4i** → **4b** → **4e** in the cases of mononucleotides **CMP** and **GMP**, and in the order of **4i** → **4b** → **4e** the cases of mononucleotides for **AMP** and **UMP**. In the 1,4-DHP molecule, the replacement of the $N_1H$ proton by methyl group reduces the binding ability of the 1,4-DHP derivative **4e** with mononucleotides, confirming the importance of the $N_1H$ group in the mechanism of this complexation. The $N_1H$ group may be involved in the formation of an intermolecular hydrogen bond, between 1,4-DHP derivatives and mononucleotide.

The largest decrease in the NMR integral intensities of the mononucleotide signals is observed for the sugar moiety. This means that most probably the binding site is phosphate group. As the integral intensities of the proton signals of purines and pyrimidines are slightly reduced, this indicates that there are hydrophobic interactions between 1,4-DHP derivatives (with long alkyl chains of the ester groups at positions 3 and 5 of the 1,4-DHP cycle) and RNA 5'-mononucleotide nitrogen bases.

To support the correct identification of the mononucleotide atoms involved in the binding process, the $^1$H NMR saturation transfer double difference (STDD) experiments were used. STDD is based on the intermolecular transfer of the magnetization from the receptor to the bound small ligands [68].

Table 10

Normalized STDD integral intensities of mononucleotide complexation with compound 4

| Comp. | | H8 | H6 | H5 | H2 | H6, H1' | H5, H1' | H1' | H2', H3' | H2' | H3' | H4' | H5' |
|---|---|---|---|---|---|---|---|---|---|---|---|---|---|
| **AMP** | **4b** | 9 | | | 15 | | | 10 | | 9 | | 36 | 21 |
| | **4e** | 2 | | | 6 | | | 9 | | 12 | | 41 | 30 |
| | **4i** | 7 | | | 15 | | | 10 | | 9 | | 31 | 28 |
| **CMP** | **4b** | | 12 | | | | 9 | | 35 | | | 24 | 21 |
| | **4e** | | 9 | | | | 3 | | 28 | | | 25 | 34 |
| | **4i** | | 11 | | | | 7 | | 32 | | | 26 | 25 |
| **GMP** | **4b** | 18 | | | | | | | | | 5 | 63 | 14 |
| | **4e** | 18 | | | | | | | | | 11 | 56 | 15 |
| | **4i** | 22 | | | | | | | | | 15 | 44 | 19 |
| **UMP** | **4b** | | | 8 | | 0 | | | | 12 | 26 | 26 | 28 |
| | **4e** | | | 0 | | 6 | | | | 2 | 25 | 32 | 36 |
| | **4i** | | | 8 | | 4 | | | | 12 | 24 | 29 | 23 |

The $^1$H STDD data show some differences in the binding of mononucleotide and compounds **4** (Table 10). The highest intensity of mononucleotide **GMP** has the H4' proton signal. For mononucleotide **AMP** the most intense signals were registered for H4' and H5' protons. In the case of **CMP** and **UMP** mononucleotides maximum intensity was observed for H3', H4' and H5' protons, indicating a stronger binding with 1,4-DHP derivatives. Despite these differences, the binding capacity of the mononucleotides to **4b** decreases in the same order (**CMP** → **UMP** → **AMP** → **GMP**), in agreement with the results of the $T_1\rho$ KMR experiments.

The binding process consists of two parts – the electrostatic attraction of the negatively charged phosphate groups and the positively charged pyridinium rings at positions 2 and 6 of the 1,4-DHP cycle (the fact that sugar ring protons are observable in the STDD spectra) and the hydrophobic interaction between the long alkyl chains and the mononucleotide heterocycles.

Despite the fact that the binding of mononucleotides and cationic lipids based on 1,4-DHP derivatives **4** is dominated by hydrophobic interactions, the NH fragment is important because

a decrease in binding activity has been observed when a proton at the nitrogen atom is replaced by a methyl group. At the same time, compound **4d** with longer alkyl chains (C16) exhibited a decrease in binding similar to the mixing of 1,4-DHP derivative **4b** with zwitterionic DPPC. The pyrimidine mononucleotide derivatives **CMP** and **UMP** were found to have higher binding activity with 1,4-DHP derivatives **4** than the purine mononucleotide derivatives **AMP** and **GMP**.

# CONCLUSIONS

1. A study of the reaction course for the bromination of 2- and 6-methyl groups of 1,4-dihydropyridine derivative with various amounts of *N*-bromosuccinimide in methanol revealed previously unknown intermediates, the structures of which were identified by NMR spectroscopy. The proposed mechanisms of the reactions have been proven on the base of NMR data and quantum chemical calculations.
2. Analysis of the structural features of the 1,4-dihydropyridine derivatives affecting the magnetic nonequivalence of the diastereotopic protons of the methylene groups at positions 2 and 6 has shown that the combined effect of magnetically anisotropic substituents and intramolecular |C-H|···O hydrogen bonds in the individual conformers leads to a considerable difference in the shielding of the methylene AB-protons.

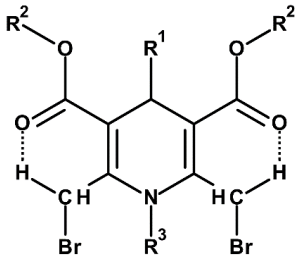

3. It has been proven that the unusual temperature dependence of the NMR signals of diastereotopic 1,4-DHP methylene group protons of positions 2 and 6 in the 1,4-dihydropyridine spectrum is caused by two conformational processes – rotation of the substituent around $C_{2,6}$-$CH_2$ and $C_{3,5}$-$CO_2$ bonds.
4. Based on the analysis of $^{1}H$, $^{13}C$, $^{15}N$ NMR and IR spectral data and the results of quantum chemical calculations, it can be concluded that 2- and 2,6-acetoxymethyl-1,4-dihydropyridine-3,5-dicarboxylates form |N-H|···O and |C-H|···O intermolecular hydrogen bonds, defining the optimal molecular structure.

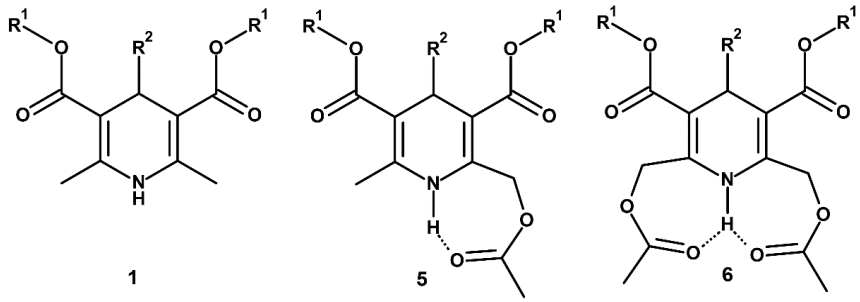

5. On the basis of quantum chemical calculations and the results of NMR spectroscopy, it has been shown that an intermolecular hydrogen bond is formed in the acetoxymethyl-1,4-DHP derivatives. In monosubstituted 2-acetoxymethyl-1,4-DHP derivatives, the $N_1H$ proton forms a five-membered H-chelate cycle with the alkoxy group oxygen, while in disubstituted 2,6-diacetoxy-methyl-1,4-DHP derivatives, the formation of two seven-membered H-chelate cycles is more favourable, that the $N_1H$

proton forms with the oxygens of the carboxyl groups of the 2- and 6- substituents of the 1,4-DHP cycle.

6. It has been shown that in the studied 1,4-dihydropyridine derivatives the downfield shift of the $N_1H$ proton in the NMR spectra, accompanied by the upfield shift of the $^{15}N$ signal and the increase of the coupling constant $^1J(^{15}N,^1H)$ values in the order **1→5→6**, indicates a decrease in the |N-H| distance if the hydrogen bond is formed. This is also confirmed by the shift of the |N-H| bond stretching band to the higher wavenumbers (blue shift) in the **1**, **5** and **6** FTIR spectra.
7. Using NMR and isothermal titration calorimetry (ITC) methods, it is possible to study the ability of the lipid-like 1,4-DHP derivatives to form complexes with 5'-mononucleotide monophosphates and to determine the dissociation constants ($K_D$) of the vesicle complexes formed.
8. Evaluation of the data obtained from ITC and NMR spectroscopy has resulted in conclusion that the binding processes between the mononucleotides and the cationic 1,4-DHP derivatives is dominated by entropic interactions.

# REFERENCES


1. Carosati, E.; Ioan, P.; Micucci, M.; Broccatelli, F.; Cruciani, G.; Zhorov, B. S.; Chiarini, A.; Budriesi, R. 1,4-Dihydropyridine Scaffold in Medicinal Chemistry, The Story So Far And Perspectives (Part 2): Action in Other Targets and Antitargets. *Curr. Med. Chem.* **2012**, *19*, 4306–4323, doi:10.2174/092986712802884204.
2. Ioan, P.; Carosati, E.; Micucci, M.; Cruciani, G.; Broccatelli, F.; S. Zhorov, B.; Chiarini, A.; Budriesi, R.; Zhorov, B. S.; Chiarini, A.; Budriesi, R. 1,4-Dihydropyridine Scaffold in Medicinal Chemistry, The Story so Far And Perspectives (Part 1): Action in Ion Channels and GPCRs. *Curr. Med. Chem.* **2011**, *18*, 4901–4922, doi:10.2174/092986711797535173.
3. WHO model list of essential medicines – 22nd list, 2021 Available online: https://www.who.int/publications/i/item/WHO-MHP-HPS-EML-2021.02.
4. Balaev, A. N.; Eleev, A. F.; Eremin, O. G.; Fedorov, V. E. Search for new drugs. *Pharm. Chem. J.* **2010**, *44*, 56–57, doi:10.1007/s11094-010-0396-7.
5. Abrego, V. H.; Martínez-Pérez, B.; Torres, L. A.; Ángeles, E.; Martínez, L.; Marroquín-Pascual, J. L.; Moya-Hernández, R.; Amaro-Recillas, H. A.; Rueda-Jackson, J. C.; Rodríguez-Barrientos, D. Antihypertensive and antiarrhythmic properties of a para-hydroxy[bis(ortho-morpholinylmethyl)]phenyl-1,4-DHP compound: Comparison with other compounds of the same kind and relationship with logP values. *Eur. J. Med. Chem.* **2010**, *45*, 4622–4630, doi:10.1016/j.ejmech.2010.07.027.
6. Hirasawa, M.; Pittman, Q. J. Nifedipine facilitates neurotransmitter release independently of calcium channels. *Proc. Natl. Acad. Sci.* **2003**, *100*, 6139–6144, doi:10.1073/pnas.0936131100.
7. Kale, S. H.; Gaware, V. M.; Chavan, P. A. Synthesis and evaluation of some new substituted 1,4-dihydro pyridine derivatives and their anticonvulsant activity. *J. Chem. Pharm. Res.* **2010**, *2*, 246–252.
8. da Costa Cabrera, D.; Santa-Helena, E.; Leal, H. P.; de Moura, R. R.; Nery, L. E. M.; Gonçalves, C. A. N.; Russowsky, D.; Montes D'Oca, M. G. Synthesis and antioxidant activity of new lipophilic dihydropyridines. *Bioorg. Chem.* **2019**, *84*, 1–16, doi:10.1016/j.bioorg.2018.11.009.
9. Andzans, Z.; Adlere, I.; Versilovskis, A.; Krasnova, L.; Grinberga, S.; Duburs, G.; Krauze, A. Effective Method of Lipase-Catalyzed Enantioresolution of 6-Alkylsulfanyl-1,4-dihydropyridines. *Heterocycles* **2014**, *89*, 43, doi:10.3987/COM-13-12839.
10. Valente, S.; Mellini, P.; Spallotta, F.; Carafa, V.; Nebbioso, A.; Polletta, L.; Carnevale, I.; Saladini, S.; Trisciuoglio, D.; Gabellini, C.; Tardugno, M.; Zwergel, C.; Cencioni, C.; Atlante, S.; Moniot, S.; Steegborn, C.; Budriesi, R.; Tafani, M.; Del Bufalo, D.; Altucci, L.; Gaetano, C.; Mai, A. 1,4-Dihydropyridines Active on the SIRT1/AMPK Pathway Ameliorate Skin Repair and Mitochondrial Function and Exhibit Inhibition of Proliferation in Cancer Cells. *J. Med. Chem.* **2016**, *59*, 1471–1491, doi:10.1021/acs.jmedchem.5b01117.
11. Briede, J.; Stivrina, M.; Vigante, B.; Stoldere, D.; Duburs, G. Acute effect of antidiabetic 1,4-dihydropyridine compound cerebrocrast on cardiac function and glucose metabolism in the isolated, perfused normal rat heart. *Cell Biochem. Funct.* **2008**, *26*, 238–245, doi:10.1002/cbf.1442.
12. Niemirowicz-Laskowska, K.; Głuszek, K.; Piktel, E.; Pajuste, K.; Durnaś, B.; Król, G.; Wilczewska, A.; Janmey, P.; Plotniece, A.; Bucki, R. Bactericidal and immunomodulatory properties of magnetic nanoparticles functionalized by 1,4-dihydropyridines. *Int. J. Nanomedicine* **2018**, *Volume 13*, 3411–3424, doi:10.2147/IJN.S157564.
13. Bruvere, I.; Bisenieks, E.; Poikans, J.; Uldrikis, J.; Plotniece, A.; Pajuste, K.; Rucins, M.; Vigante, B.; Kalme, Z.; Gosteva, M.; Domracheva, I.; Velena, A.; Vukovic, T.;

Milkovic, L.; Dubur, G.; Zarkovic, N. Dihydropyridine Derivatives as Cell Growth Modulators In Vitro. *Oxid. Med. Cell. Longev.* **2017**, *2017*, 1–15, doi:10.1155/2017/4069839.
14. Hjemdahl, P.; Wallen, N. H. Calcium antagonist treatment, sympathetic activity and platelet function. *Eur. Heart J.* **1997**, *18*, 36–50, doi:10.1093/eurheartj/18.suppl_A.36.
15. Li, A.-H.; Chang, L.; Ji, X.; Melman, N.; Jacobson, K. A. Functionalized Congeners of 1,4-Dihydropyridines as Antagonist Molecular Probes for A 3 Adenosine Receptors. *Bioconjug. Chem.* **1999**, *10*, 667–677, doi:10.1021/bc9900136.
16. Cindric, M.; Cipak, A.; Serly, J.; Plotniece, A.; Jaganjac, M.; Mrakovcic, L.; Lovakovic, T.; Dedic, A.; Soldo, I.; Dubur, G.; Zarkovic, N.; Molnár, J. Reversal of multidrug resistance in murine lymphoma cells by amphiphilic dihydropyridine antioxidant derivative. *Anticancer Res.* **2010**, *30*, 4063–4069.
17. Pajuste, K.; Hyvönen, Z.; Petrichenko, O.; Kaldre, D.; Rucins, M.; Cekavicus, B.; Ose, V.; Skrivele, B.; Gosteva, M.; Morin-Picardat, E.; Plotniece, M.; Sobolev, A.; Dubur, G.; Ruponen, M.; Plotniece, A. Gene delivery agents possessing antiradical activity: self-assembling cationic amphiphilic 1,4-dihydropyridine derivatives. *New J. Chem.* **2013**, *37*, 3062, doi:10.1039/c3nj00272a.
18. Giorgi, G.; Adamo, M. F. A.; Ponticelli, F.; Ventura, A. Synthesis, structural and conformational properties, and gas phase reactivity of 1,4-dihydropyridine ester and ketone derivatives. *Org. Biomol. Chem.* **2010**, *8*, 5339, doi:10.1039/c0ob00494d.
19. Hyvönen, Z.; Plotniece, A.; Reine, I.; Chekavichus, B.; Dubur, G.; Urtti, A. Novel cationic amphiphilic 1,4-dihydropyridine derivatives for DNA delivery. *Biochim. Biophys. Acta – Biomembr.* **2000**, *1509*, 451–466, doi:10.1016/S0005-2736(00)00327-8.
20. Alix, A.; Lalli, C.; Retailleau, P.; Masson, G. Highly enantioselective electrophilic α-bromination of enecarbamates: chiral phosphoric acid and calcium phosphate salt catalysts. *J. Am. Chem. Soc.* **2012**, *134*, 10389–10392, doi:10.1021/ja304095z.
21. Skrastin'sh, I. P.; Liepin'sh, E. E.; Kastron, V. V.; Dubur, G. Y. Y. Reactions of N-chlorosuccinimide with 4-phenyl-1,4-dihydropyridines. *Chem. Heterocycl. Compd.* **1990**, *26*, 421–424, doi:10.1007/BF00497214.
22. Jaguar, Schrödinger, LLC, New York, NY, 2011.
23. Pajuste, K.; Plotniece, A.; Kore, K.; Intenberga, L.; Cekavicus, B.; Kaldre, D.; Dubur, G.; Sobolev, A. Use of pyridinium ionic liquids as catalysts for the synthesis of 3,5-bis(dodecyloxycarbonyl)-1,4-dihydropyridine derivative. *Open Chem.* **2011**, *9*, 143–148, doi:10.2478/s11532-010-0132-x.
24. Plotniece, A.; Pajuste, K.; Kaldre, D.; Cekavicus, B.; Vigante, B.; Turovska, B.; Belyakov, S.; Sobolev, A.; Dubur, G. Oxidation of cationic 1,4-dihydropyridine derivatives as model compounds for putative gene delivery agents. *Tetrahedron* **2009**, *65*, 8344–8349, doi:10.1016/j.tet.2009.08.012.
25. Skrastin'sh, I. P.; Kastron, V. V.; Chekavichus, B. S.; Sausin'sh, A. é. é. E.; Zolotoyabko, R. M.; Dubur, G. Y. Y. Bromination of 4-aryl-3,5-dialkoxycarbonyl-2,6-dimethyl-1,4-dihydropyridines. *Chem. Heterocycl. Compd.* **1991**, *27*, 989–994, doi:10.1007/BF00484364.
26. Ozolins, R.; Plotniece, M.; Pajuste, K.; Putralis, R.; Pikun, N.; Sobolev, A.; Plotniece, A.; Rucins, M. 1,1′-{[3,5-Bis((dodecyloxycarbonyl)-4-phenyl-1,4-dihydropyridine-2,6-diyl]bis(methylene)}bis[4-(anthracen-9-yl)pyridin-1-ium] Dibromide. *Molbank* **2022**, *2022*, M1438, doi:10.3390/M1438.
27. Petrichenko, O.; Plotniece, A.; Pajuste, K.; Rucins, M.; Dimitrijevs, P.; Sobolev, A.; Sprugis, E.; Cēbers, A. Evaluation of Physicochemical Properties of Amphiphilic 1,4-Dihydropyridines and Preparation of Magnetoliposomes. *Nanomaterials* **2021**, *11*, 593, doi:10.3390/nano11030593.
28. Muhamadejevs, R. Uz 1,4-dihidropiridīnu bāzes veidotu katjono vezikulu pētīšana ar KMR metodēm. Maģistra darbs, Rīgas Tehniskā universitāte, Materiālzinātnes un

lietišķās ķīmijas fakultāte, 2012, https://ndr.rtu.lv/lv/view/6382/.
29. Petrova, M.; Muhamadejev, R.; Vigante, B.; Cekavicus, B.; Plotniece, A.; Duburs, G.; Liepinsh, E. Intramolecular C-H···O hydrogen bonding in 1,4-dihydropyridine derivatives. *Molecules* **2011**, *16*, 8041–8052, doi:10.3390/molecules16098041.
30. Görlitzer, K.; Bartke, U.; Schmidt, E. Zur Reaktion von Nifedipin mit Pyridiniumbromidperbromid. *Arch. Pharm. (Weinheim).* **1991**, *324*, 105–109, doi:10.1002/ardp.19913240209.
31. Секацис И.П.; Лиепиньш, Э. Э.; Дубур, Г. Я. Конформационная подвижность 1,4-дигидропиридинов. *Изв. АН ЛатвССР. Сер. хим.* **1979**, *1*, 111–112.
32. Mazzanti, A.; Drakopoulos, A.; Christina, T.; Kolocouris, A. Rotation Barriers of 1-Adamantyl-Csp 3 Bonds Measured with Dynamic NMR. *ChemistrySelect* **2019**, *4*, 7645–7648, doi:10.1002/slct.201901042.
33. Goba, I.; Turovska, B.; Belyakov, S.; Liepinsh, E. Synthesis, spectroscopic and conformational analysis of 1,4-dihydroisonicotinic acid derivatives. *J. Mol. Struct.* **2014**, *1074*, 549–558, doi:10.1016/j.molstruc.2014.06.044.
34. Feller, D.; Craig, N. C. High Level ab Initio Energies and Structures for the Rotamers of 1,3-Butadiene. *J. Phys. Chem. A* **2009**, *113*, 1601–1607, doi:10.1021/jp8095709.
35. Gellman, S. H.; Dado, G. P.; Liang, G. B.; Adams, B. R. Conformation-directing effects of a single intramolecular amide-amide hydrogen bond: variable-temperature NMR and IR studies on a homologous diamide series. *J. Am. Chem. Soc.* **1991**, *113*, 1164–1173, doi:10.1021/ja00004a016.
36. Ishikawa, R.; Kojima, C.; Ono, A.; Kainosho, M. Developing model systems for the NMR study of substituent effects on the N-H...N hydrogen bond in duplex DNA. *Magn. Reson. Chem.* **2001**, *39*, S159–S165, doi:10.1002/mrc.941.
37. Del Bene, J. E.; Elguero, J. Systematic ab Initio Study of 15 N− 15 N and 15 N− 1 H Spin−Spin Coupling Constants Across N−H + −N Hydrogen Bonds: Predicting N−N and N−H Coupling Constants and Relating Them to Hydrogen Bond Type. *J. Phys. Chem. A* **2006**, *110*, 7496–7502, doi:10.1021/jp0613642.
38. Contreras, R. Angular dependence of spin–spin coupling constants. *Prog. Nucl. Magn. Reson. Spectrosc.* **2000**, *37*, 321–425, doi:10.1016/S0079-6565(00)00027-3.
39. Joseph, J.; Jemmis, E. D. Red-, Blue-, or No-Shift in Hydrogen Bonds: A Unified Explanation. *J. Am. Chem. Soc.* **2007**, *129*, 4620–4632, doi:10.1021/ja067545z.
40. Ghosh, S.; Wategaonkar, S. C–H···Y (Y=N, O, π) Hydrogen Bond: A Unique Unconventional Hydrogen Bond. *J. Indian Inst. Sci.* **2020**, *100*, 101–125, doi:10.1007/s41745-019-00145-5.
41. Contreras, R. H.; Peralta, J. E.; Giribet, C. G.; Ruiz de azúa, M. C.; Facelli, J. C. Advances in theoretical and physical aspects of spin-spin coupling constants. In *Annual Reports on NMR Spectroscopy*; PublisherAcademic Press Inc., 2000; Vol. 41, pp. 55–184 ISBN 012505341X.
42. Goba, I.; Liepinsh, E. 15 N NMR of 1,4-dihydropyridine derivatives. *Magn. Reson. Chem.* **2013**, *51*, 391–396, doi:10.1002/mrc.3959.
43. Kyogoku, Y. Application of 15 N NMR Spectroscopy to Studies of the Intermolecular Interaction of Biomolecules. *Appl. Spectrosc. Rev.* **1981**, *17*, 279–335, doi:10.1080/05704928108060407.
44. Bagheri, S.; Masoodi, H. R.; Abadi, M. N. Estimation of individual NH···X (X = N, O) hydrogen bonding energies in some complexes involving multiple hydrogen bonds using NBO calculations. *Theor. Chem. Acc.* **2015**, *134*, 127, doi:10.1007/s00214-015-1738-z.
45. Kuroki, S.; Ando, S.; Ando, I.; Shoji, A.; Ozaki, T.; Webb, G. A. Hydrogen-bonding effect on 15N NMR chemical shifts of the glycine residue of oligopeptides in the solid state as studied by high-resolution solid-state NMR spectroscopy. *J. Mol. Struct.* **1990**, *240*, 19–29, doi:10.1016/0022-2860(90)80492-3.
46. Witanowski, M.; Stefaniak, L.; Webb, G. A. Nitrogen NMR Spectroscopy. In *Annual Reports on NMR Spectroscopy*; 1982; Vol. 7, pp. 1–486, ISBN 9780125053181.

47. Dziembowska, T.; Hansen, P. E.; Rozwadowski, Z. Studies based on deuterium isotope effect on 13C chemical shifts. *Prog. Nucl. Magn. Reson. Spectrosc.* **2004**, *45*, 1–29, doi:10.1016/j.pnmrs.2004.04.001.
48. Sobczyk, L.; Obrzud, M.; Filarowski, A. H/D Isotope Effects in Hydrogen Bonded Systems. *Molecules* **2013**, *18*, 4467–4476, doi:10.3390/molecules18044467.
49. Buncel, E.; Jones, J. R. *Isotopes in the Physical and Biomedical Sciences: Isotopic applications in NMR studies*; Isotopes in the Physical and Biomedical Sciences; Elsevier Science Publishes, 1991; ISBN 9780444890900.
50. Frisch, M. J.; Trucks, G. W.; Schlegel, H. B.; Scuseria, G. E.; Robb, M. A.; Cheeseman, J. R.; Scalmani, G.; Barone, V.; Mennucci, B.; Petersson, G. A.; Nakatsuji, H.; Caricato, M.; Li, X.; Hratchian, H. P.; Izmaylov, A. F.; Bloino, J.; Zheng, G.; Sonnenberg, J. L.; Hada, M.; Ehara, M.; Toyota, K.; Fukuda, R.; Hasegawa, J.; Ishida, M.; Nakajima, T.; Honda, Y.; Kitao, O.; Nakai, H.; Vreven, T.; Montgomery, J. A.; Peralta, J. E.; Ogliaro, F.; Bearpark, M.; Heyd, J. J.; Brothers, E.; Kudin, K. N.; Staroverov, V.; Keith, T.; Kobayashi, R.; Normand, J.; Raghavachari, K.; Rendell, A.; Burant, J. C.; Iyengar, S. S.; Tomasi, J.; Cossi, M.; Rega, N.; Millam, J. M.; Klene, M.; Knox, J. E.; Cross, J. B.; Bakken, V.; Adamo, C.; Jaramillo, J.; Gomperts, R.; Stratmann, R. E.; Yazyev, O.; Austin, A. J.; Cammi, R.; Pomelli, C.; Ochterski, J. W.; Martin, R. L.; Morokuma, K.; Zakrzewski, V. G.; Voth, G. A.; Salvador, P.; Dannenberg, J. J.; Dapprich, S.; Daniels, A. D.; Farkas, Ö.; Foresman, J. B.; Ortiz, J. V; Cioslowski, J.; Fox, D. J. Gaussian 09, Revision D.01. *Gaussian 09, Revis. D.01, Gaussian, Inc., Wallingford, CT 06492, USA* 2013.
51. Apsite, G.; Timofejeva, I.; Vezane, A.; Vigante, B.; Rucins, M.; Sobolev, A.; Plotniece, M.; Pajuste, K.; Kozlovska, T.; Plotniece, A. Synthesis and Comparative Evaluation of Novel Cationic Amphiphile C12-Man-Q as an Efficient DNA Delivery Agent In Vitro. *Molecules* **2018**, *23*, 1540, doi:10.3390/molecules23071540.
52. Petrichenko, O.; Rucins, M.; Vezane, A.; Timofejeva, I.; Sobolev, A.; Cekavicus, B.; Pajuste, K.; Plotniece, M.; Gosteva, M.; Kozlovska, T.; Plotniece, A. Studies of the physicochemical and structural properties of self-assembling cationic pyridine derivatives as gene delivery agents. *Chem. Phys. Lipids* **2015**, *191*, 25–37, doi:10.1016/j.chemphyslip.2015.08.005.
53. Schumaker, K. S.; Gizinski, M. J. G Proteins Regulate Dihydropyridine Binding to Moss Plasma Membranes. *J. Biol. Chem.* **1996**, *271*, 21292–21296, doi:10.1074/jbc.271.35.21292.
54. Textor, M.; Keller, S. Automated analysis of calorimetric demicellization titrations. *Anal. Biochem.* **2015**, *485*, 119–121, doi:10.1016/j.ab.2015.06.009.
55. Jungnickel, C.; Łuczak, J.; Ranke, J.; Fernández, J.; Müller, A.; Thöming, J. Micelle formation of imidazolium ionic liquids in aqueous solution. *Colloids Surfaces A Physicochem. Eng. Asp.* **2008**, *316*, 278–284, doi:10.1016/j.colsurfa.2007.09.020.
56. Ottaviani, G.; Wendelspiess, S.; Alvarez-Sánchez, R. Importance of critical micellar concentration for the prediction of solubility enhancement in biorelevant media. *Mol. Pharm.* **2015**, *12*, 1171–9, doi:10.1021/mp5006992.
57. Fisicaro, E.; Compari, C.; Duce, E.; Biemmi, M.; Peroni, M.; Braibanti, A. Thermodynamics of micelle formation in water, hydrophobic processes and surfactant self-assemblies. *Phys. Chem. Chem. Phys.* **2008**, *10*, 3903, doi:10.1039/b719630j.
58. Fielding, L. NMR Methods for the Determination of Protein- Ligand Dissociation Constants. *Curr. Top. Med. Chem.* 2003, *3*, 39–53.
59. Leavitt, S.; Freire, E. Direct measurement of protein binding energetics by isothermal titration calorimetry. *Curr. Opin. Struct. Biol.* **2001**, *11*, 560–566, doi:10.1016/S0959-440X(00)00248-7.
60. Baranauskiene, L.; Petrikaite, V.; Matuliene, J.; Matulis, D. Titration calorimetry standards and the precision of isothermal titration calorimetry data. *Int. J. Mol. Sci.* **2009**, *10*, 2752–2762, doi:10.3390/ijms10062752.

61. Salim, N. N.; Feig, A. L. Isothermal titration calorimetry of RNA. *Methods* **2009**, *47*, 198–205, doi:10.1016/j.ymeth.2008.09.003.
62. Sessler, J. L.; Gross, D. E.; Cho, W.-S.; Lynch, V. M.; Schmidtchen, F. P.; Bates, G. W.; Light, M. E.; Gale, P. A. Calix[4]pyrrole as a Chloride Anion Receptor: Solvent and Countercation Effects. *J. Am. Chem. Soc.* **2006**, *128*, 12281–12288, doi:10.1021/ja064012h.
63. Frasca, V. Biophysical characterization of antibodies with isothermal titration calorimetry. *J. Appl. Bioanal.* **2016**, *2*, 90–102, doi:10.17145/jab.16.013.
64. Matulis, D.; Rouzina, I.; Bloomfield, V. A. Thermodynamics of Cationic Lipid Binding to DNA and DNA Condensation: Roles of Electrostatics and Hydrophobicity. *J. Am. Chem. Soc.* **2002**, *124*, 7331–7342, doi:10.1021/ja0124055.
65. Cassidy, L. M.; Burcar, B. T.; Stevens, W.; Moriarty, E. M.; McGown, L. B. Guanine-Centric Self-Assembly of Nucleotides in Water: An Important Consideration in Prebiotic Chemistry. *Astrobiology* **2014**, *14*, 876–886, doi:10.1089/ast.2014.1155.
66. Eimer, W.; Dorfmueller, T. Self-aggregation of guanosine 5'-monophosphate, studied by dynamic light scattering techniques. *J. Phys. Chem.* **1992**, *96*, 6790–6800, doi:10.1021/j100195a048.
67. Meyer, B.; Peters, T. NMR Spectroscopy Techniques for Screening and Identifying Ligand Binding to Protein Receptors. *Angew. Chemie Int. Ed.* **2003**, *42*, 864–890, doi:10.1002/anie.200390233.
68. Mayer, M.; Meyer, B. Characterization of Ligand Binding by Saturation Transfer Difference NMR Spectroscopy. *Angew. Chemie Int. Ed.* **1999**, *38*, 1784–1788, doi:10.1002/(SICI)1521-3773(19990614)38:12<1784::AID-ANIE1784>3.0.CO;2-Q.

**Ruslans Muhamadejevs** was born in Liepaja, in 1987. He received a Bachelor's degree in Chemistry and a Master's degree of Engineering Science in Nanotechnologies from Riga Technical University in 2010 and 2012, respectively. Since 2007, has worked in the Laboratory of Physical Organic Chemistry of Latvian Institute of Organic Synthesis, focusing his research on nuclear magnetic resonance and computational chemistry. He has co-authored sixteen original publications indexed in *Scopus* and *Web of Science* databases. Currently, he is a Research Assistant in the Latvian Institute of Organic Synthesis.